PREDICTION OF THE CONFORMATION OF THE HISTONES

GERALD D. FASMAN, PETER Y. CHOU, *and* ALICE J. ADLER

From the Graduate Department of Biochemistry, Brandeis University, Waltham, Massachusetts 02154

ABSTRACT The secondary structures of the histones, H1, H2A, H2B, H3, and H4 have been predicted utilizing the predictive scheme of Chou and Fasman (*Biochemistry* **13**:211, 222 [1974]) and a new set of conformational parameters based on the X-ray data of 29 protein structures. The α-helical, β-sheet, reverse β-turns, and random coil regions of these proteins are carefully delineated. Structures are specified which are most probable under various environmental conditions, i.e., for changes in ionic strength, association between histones and in association with DNA. Potential conformational changes within these histones are also predicted.

INTRODUCTION

The control of gene regulation through the manipulation of the conformation of the nucleoprotein complex of the nucleus, chromatin, has been receiving wide attention. (For reviews see Fitzsimons and Wolstenholme, 1975; Elgin and Weintraub, 1975; Elgin et al., 1971.) The histones, one component of chromatin, have been widely studied, as individual components, as organized complexes (Van Holde and Isenberg, 1975; Kornberg and Thomas, 1974), and for information on the association of these complexes along the DNA chain (Olins and Olins, 1974; Kornberg, 1974; Lohr and Van Holde, 1975).

The prediction of protein conformation has made significant progress in recent years. Chou and Fasman (1974*a*,*b*) have computed the conformational parameters for the 20 amino acids in the α-helix, β-sheet, reverse β-turn,[1] and random coil regions in 15 proteins of known X-ray structure, and have formulated a new predictive model for elucidating protein secondary structures with 80% accuracy. By means of this formulation, the conformations of the *lac* repressor (Chou et al., 1975), glucagon (Chou and Fasman, 1975), the coenzyme-binding domains of glutamate dehydrogenases (Wootton, 1974), proinsulins (Snell and Smyth, 1975), and fd gene 5 DNA-binding protein (Anderson et al., 1975) have been proposed. In addition, experimental studies showed a correlation of the helical forming potential of synthetic ribonuclease-S-(1-20)

[1] A β-turn consists of four amino acids in a region where the protein chain folds back on itself by nearly 180°, with the $C_i^\alpha - C_{i+3}^\alpha$ distance below 7 Å, as well as possible hydrogen bonding between the CO group of residue i and the NH group of residue i + 3, if the $O_i - N_{i+3}$ distance is below 3.5 Å.

TABLE I

CONFORMATIONAL PARAMETERS FOR HELICAL AND β-SHEET RESIDUES BASED ON 29 PROTEINS*

Helical residues‡	P_α		β-sheet residues§	P_β	
$Glu^{(-)}$	1.51	H_α	Val	1.70	H_β
Met	1.45		Ile	1.60	
Ala	1.42		Tyr	1.47	
Leu	1.21		Phe	1.38	h_β
$Lys^{(+)}$	1.16	h_α	Trp	1.37	
Phe	1.13		Leu	1.30	
Gln	1.11		Cys	1.19	
Trp	1.08		Thr	1.19	
Ile	1.08		Gln	1.10	
Val	1.06		Met	1.05	
$Asp^{(-)}$	1.01	I_α	$Arg^{(+)}$	0.93	i_β
$His^{(+)}$	1.00		Asn	0.89	
$Arg^{(+)}$	0.98	i_α	$His^{(+)}$	0.87	
Thr	0.83		Ala	0.83	
Ser	0.77		Ser	0.75	b_β
Cys	0.70	b_α	Gly	0.75	
Tyr	0.69		$Lys^{(+)}$	0.74	
Asn	0.67		Pro	0.55	
Pro	0.57	B_α	$Asp^{(-)}$	0.54	B_β
Gly	0.57		$Glu^{(-)}$	0.37	

*Chou and Fasman (to be published).

†Helical assignments: H_α, strong α-former; h_α, α-former; I_α, weak α-former; i_α, α-indifferent; b_α, α-breaker; B_α, strong α-breaker. I_α assignments are also given to Pro (near the N-terminal helix) and to Arg (near the C-terminal helix).

§β-sheet assignments: H_β, strong β-former; h_β, β-former; i_β, β-indifferent; b_β, β-breaker; B_β, strong β-breaker.

peptides with binding to the S-protein (Dunn and Chaiken, 1975). Furthermore, the efficacy of different predictive methods has been tested in predicting the conformation of adenylate kinase (Schulz et al., 1974) and T4 phage lysozyme (Matthews, 1975). Recently, the authors have reevaluated the conformational parameters based on the X-ray data of 29 proteins (Chou and Fasman, to be published) which are listed in Table I.

This paper utilizes these new parameters to predict the conformation of the five histones, and suggests possible conformational transitions induced by environmental changes, as well as histone-histone and DNA-histone interactions. Other predictive schemes have been applied to the histones by various workers. The results of these predictions are compared with the present analysis in a more comprehensive paper (Fasman et al., 1976).

RESULTS AND DISCUSSION

H1: Prediction of Secondary Structure

The complete sequence of a single H1 polypeptide has yet to be published. However, the NH_2-terminus of rabbit thymus H1 (residues 1–106) has been completed by Cole

H1 RABBIT THYMUS 91-106)
TROUT TESTIS (107-205)

205 AMINO ACID RESIDUES

```
  1   2   3   4   5   6   7   8   9  10  11  12  13  14  15
SER- GLU- ALA- PRO- ALA- GLU- THR- ALA- ALA- PRO- ALA- PRO- ALA- GLU- LYS-

 16  17  18  19  20  21  22  23  24  25  26  27  28  29  30
SER- PRO- ALA- LYS- LYS- LYS- LYS- ALA- ALA- LYS- LYS- PRO- GLY- ALA- GLY-

 31  32  33  34  35  36  37  38  39  40  41  42  43  44  45
ALA- ALA- LYS- ARG- LYS- ALA- ALA- GLY- PRO- PRO- VAL- SER- GLU- LEU- ILE-

 46  47  48  49  50  51  52  53  54  55  56  57  58  59  60
THR- LYS- ALA- VAL- ALA- ALA- SER- LYS- GLU- ARG- ASN- GLY- LEU- SER- LEU-

 61  62  63  64  65  66  67  68  69  70  71  72  73  74  75
ALA- ALA- LEU- LYS- LYS- ALA- LEU- ALA- ALA- GLY- GLY- TYR- ASP- VAL- GLU-

 76  77  78  79  80  81  82  83  84  85  86  87  88  89  90
LYS- ASN- ASN- SER- ARG- ILE- LYS- LEU- GLY- LEU- LYS- SER- LEU- VAL- SER-

 91  92  93  94  95  96  97  98  99 100 101 102 103 104 105
LYS- GLY- THR- LEU- VAL- GLU- THR- LYS- GLY- THR- GLY- ALA- SER- GLY- SER-

106 107 108 109 110 111 112 113 114 115 116 117 118 119 120
PHE- LYS- LYS- LEU- ASN- LYS- LYS- ALA- VAL- GLU- ALA- LYS- LYS- PRO- ALA-

121 122 123 124 125 126 127 128 129 130 131 132 133 134 135
LYS- LYS- ALA- ALA- ALA- PRO- LYS- ALA- LYS- LYS- VAL- ALA- ALA- LYS- LYS-

136 137 138 139 140 141 142 143 144 145 146 147 148 149 150
PRO- ALA- ALA- ALA- LYS- LYS- PRO- LYS- LYS- VAL- ALA- ALA- LYS- LYS- ALA-

151 152 153 154 155 156 157 158 159 160 161 162 163 164 165
VAL- ALA- ALA- LYS- LYS- SER- PRO- LYS- LYS- ALA- LYS- LYS- PRO- ALA- THR-

166 167 168 169 170 171 172 173 174 175 176 177 178 179 180
PRO- LYS- LYS- ALA- ALA- LYS- SER- PRO- LYS- LYS- ALA- THR- LYS- ALA- ALA-

181 182 183 184 185 186 187 188 189 190 191 192 193 194 195
LYS- PRO- LYS- ALA- ALA- LYS- PRO- LYS- LYS- ALA- ALA- LYS- SER- PRO- LYS-

196 197 198 199 200 201 202 203 204 205
LYS- VAL- LYS- LYS- PRO- ALA- ALA- ALA- LYS- LYS-
```

FIGURE 1 The amino acid sequence of histone H1. From rabbit thymus (residues 1–106) as determined by Cole et al. combined with trout testis (residues 107–205) sequenced by G. H. Dixon (private communication).

et al. (Jones et al., 1974; Rall and Cole, 1971), and the COOH-terminus of the trout testis histone (107–205) has been sequenced by G. H. Dixon (private communication). These two partial sequences have been combined as a "model H1" sequence which is given in Fig. 1. Application of the conformational parameters from 29 proteins and the rules previously formulated (Chou and Fasman, 1974*a, b*) to the H1 sequence yields

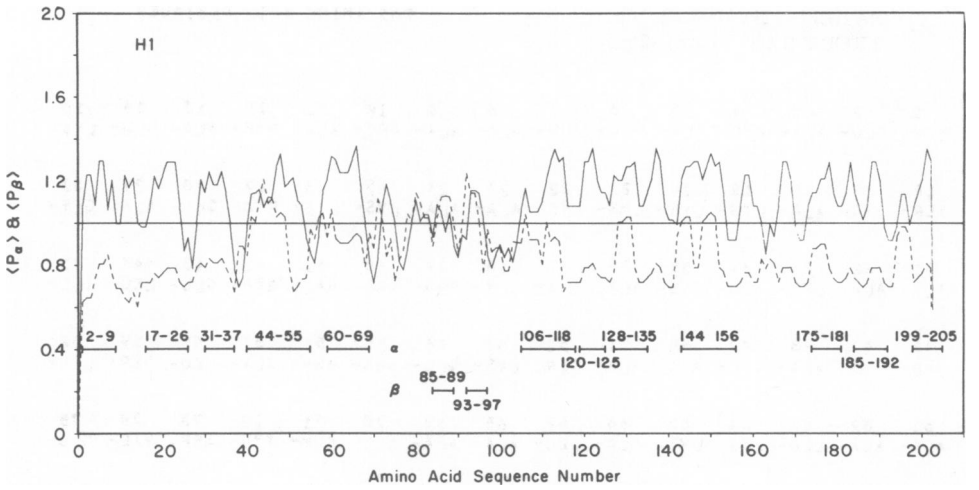

FIGURE 2 The conformational profile of H1. Based on the P_α and P_β values of 29 proteins (Chou and Fasman, to be published). The helical potential $<P_\alpha>$ (——) at residue i is the sum of the P_α values of residues i to i + 3 divided by 4. The β-sheet potential of $<P_\beta>$ (- - - -) is determined in a similar manner by averaging the P_β values of residues i to i + 3. Regions with helical and β-sheet forming potential lie above the cut-off point $<P_\alpha> = <P_\beta> = 1.0$ with tetrapeptide breakers falling below 1.0. The predicted α- and β-regions are underlined.

the conformational profile of the α-helical and β-sheet regions seen in Fig. 2. The predicted α-helix, β-sheet, and coil regions for H1 are summarized in Table II. The relative composition of the conformational regions are: α-helix 55%, β-sheet 5%, and 40% random (unstructured region) and/or β-turns. There are 12 helical regions, composed of 112 residues, only two β-sheet sections containing 10 residues, and the remaining 83 residues, in the random or β-turn conformation. The relative probability that a tetrapeptide will form a β-turn is depicted in the probability profile shown in Fig. 3. The summation of this profile is displayed in Table II, showing 15 specific β-turns, or 29% of the H1 molecule, thus only 11% of the structure is predicted to be unstructured.

The complete predicted secondary structure of histone H1 is represented in the schematic diagram, Fig. 4. The two β-sheet regions (85–89) and (93–97) have a predicted β-turn of high probability (see Fig. 3) between them (90–93), so that anti-parallel β-sheet formation is favored in this region. The remaining α-helical regions are widely distributed throughout the chain, although there are two stretches of the chain [residues (70–105) and (157–174)] totally devoid of helices.

The uneven distribution of amino acid residues in the histones has frequently been commented on (Delange et al., 1969; Ogawa et al., 1969; Iwai et al., 1970; Bustin et al., 1969), and specific functions of the basic and hydrophobic regions have been proposed. The distribution of the charged groups and hydrophobic regions are shown in Fig. 5, and is similar to the plots of Van Holde and Isenberg (1975) with the exception that the present plot includes His as a positively charged residue (at pH 7.0). It can be seen that for H1 there is a concentration of positive charges in residues (15–26), there is a cluster

TABLE II

CONFORMATIONAL PREDICTION OF H1 COMPUTED FOR HELIX, β-SHEET, AND β-TURN REGIONS: $<P_\alpha>$, $<P_\beta>$, AND $<P_t>$ VALUES

H1	Rabbit thymus (residues 1–106)/trout testis (residues 107–205)		
	Region*	$<P_\alpha>$†	$<P_\beta>$†
Helix	2–9 (8)	1.26	0.73
	17–26 (10)	1.18	0.75
	31–37 (7)	1.28	0.82
	41–55 (15)	1.16	0.98
	60–69 (10)	1.30	0.95
	106–118 (13)	1.18	0.90
	120–125 (6)	1.33	0.80
	128–135 (8)	1.25	0.89
	144–156 (13)	1.21	0.92
	175–181 (7)	1.22	0.84
	185–192 (8)	1.18	0.75
	199–205 (7)	1.19	0.75
β-sheet	85–89 (5)	1.08	1.16
	93–97 (5)	1.09	1.15

β-turn§	Tetrapeptide	$<P_t>$†	$<P_\alpha>$†	$<P_\beta>$†
9–12‖	Ala-Pro-Ala-Pro	1.09	1.00	0.69
26–29	Lys-Pro-Gly-Ala	1.19	0.93	0.72
38–41‖	Gly-Pro-Pro-Val	1.27	0.69	0.89
55–58	Arg-Asn-Gly-Leu	1.16	0.86	0.97
69–72	Ala-Gly-Gly-Tyr	1.23	0.81	0.95
77–80	Asn-Asn-Ser-Arg	1.37	0.77	0.87
90–93	Ser-Lys-Gly-Thr	1.24	0.83	0.86
97–100	Thr-Lys-Gly-Thr	1.12	0.85	0.97
102–105	Ala-Ser-Gly-Ser	1.27	0.88	0.77
125–128**	Ala-Pro-Lys-Ala	0.96	1.14	0.74
141–144	Lys-Pro-Lys-Lys	1.13	1.01	0.69
156–159	Ser-Pro-Lys-Lys	1.24	0.91	0.70
165–168	Thr-Pro-Lys-Lys	1.12	0.93	0.80
172–175	Ser-Pro-Lys-Lys	1.24	0.91	0.70
193–196	Ser-Pro-Lys-Lys	1.24	0.91	0.70
Helix: 55%	β-turns: 29%			
β-sheet: 5%	Coil: 11%			

*The predicted helix and β-sheet regions are based on the rules of Chou and Fasman (1974*b*) with conformational parameters updated for 29 proteins.

† $<P_\alpha>$, $<P_\beta>$, $<P_t>$ are, respectively, the average conformational potential for the computed region to be in the helical, β-sheet, and β-turn conformation.

§Based on the probability profile of Fig. 3.

‖ β-turns are predicted at positions 9–12 and 38–41 due to the two Pro residues in these tetrapeptides and their $<P_t>$ values, even though their P_t values were close to average ($<P_t> = 5 \times 10^{-5}$).

**Tetrapeptide 125–128 is predicted as a β-turn despite $<P_\alpha> > <P_t>$ since Pro 126 forms the link between two helices, thus accounting for the high $<P_\alpha>$ value at this position.

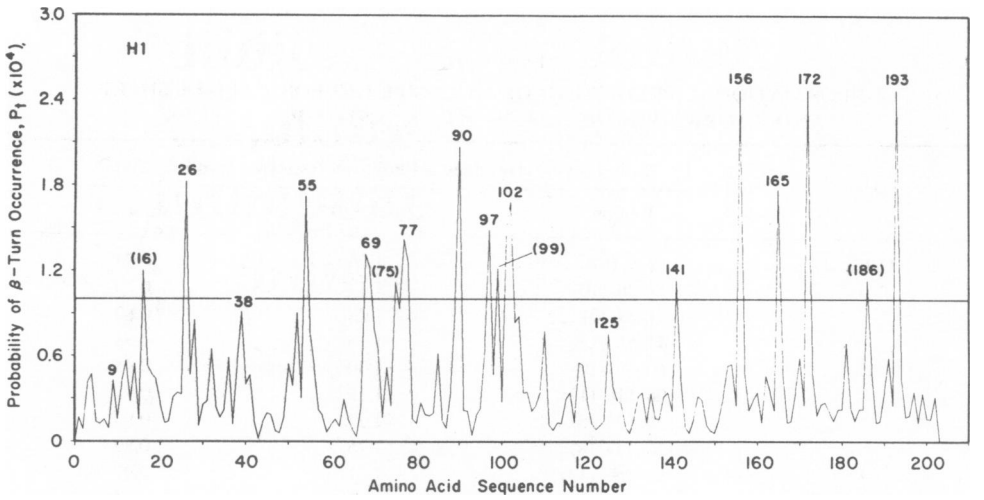

FIGURE 3 Probability of tetrapeptide β-turns in H1. The horizontal line corresponds to an arbitrary cut-off value of 1.0×10^{-4} which is double the average probability of β-turn occurrence ($<p_t> = 0.5 \times 10^{-4}$) in 29 proteins (Chou and Fasman, to be published). Of the 16 sharp peaks above the cut-off, 12 were predicted as β-turns, while 4 were excluded (residue number shown in parentheses) as belonging to other regions. Three peaks below the cut-off were predicted as β-turns for reasons explained in Table I.

of positive charges in residues (106–122) and there are 14 clusters of two adjacent positive charges in the sequence (122–205). Thus the helices predicted for (17–26) and (31–37) carry several adjacent basic charges, which should be unfavorable due to charge repulsion. The reason for the predicted helices in these regions is due to the helical potential of lysine residues in proteins ($P_\alpha = 1.16$) since proteins generally do not have clusters of positively charged residues. Thus the prediction for H1 is the maximal structural potential found for the various conformations, and may only occur when histones are found under environmental conditions where charge repulsion is minimized, either due to intrapolypeptide folding, histone-histone interactions, and/or when combined with DNA in chromatin. In the latter case, by neutralizing the positive charges upon complexation with the DNA-phosphates, the cluster of lysines in H1 could potentially assume the predicted helical conformation.

It is interesting to note the heavy clusters of positively charged residues and the total absence of negatively charged residues at the N-terminal chains of histones H2A (1–40), H2B (1–24), H3 (1–49), and H4 (1–23). In contrast, H1 has three negatively charged residues and no positive charges in the N-terminal sequence (1–14), while the C-terminal sequence (116–205) is heavily populated with positively charged residues and totally devoid of negative charges. H1 did not show any potential for conformational changes.

The prediction discussed above allowed for the *maximal* helical structure. However, it has been shown that consideration of electrostatic interactions can destabilize helices, while hydrophobic interactions can offer additional stabilization.

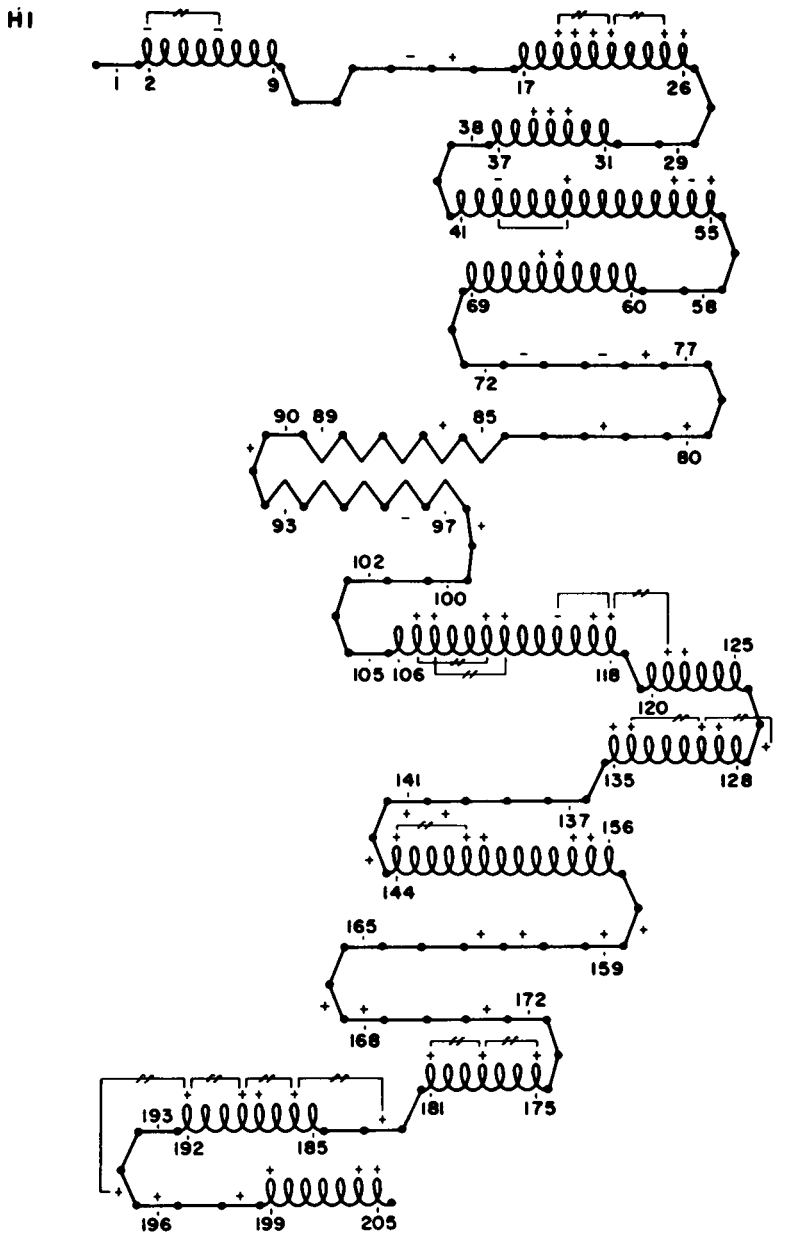

FIGURE 4 Schematic diagram of the secondary structure predicted for H1. Residues are represented in helical (ℓ), β-sheet ($\wedge$), and coil (——) conformational states. Chain reversals denote β-turn tetrapeptides. The positions of charged residues are indicated, and conformation boundary residues are numbered. Electrostatic interactions between i ± 3 and i ± 4 charged residues in helices are denoted as (—) for charge neutralization and (⌐ʃʃ¬) for charge repulsion. Helices with (⌐ʃʃ¬) will be disrupted at low ionic strength, but may be stabilized at high ionic strength or upon interaction with DNA phosphates where charge repulsion is minimized.

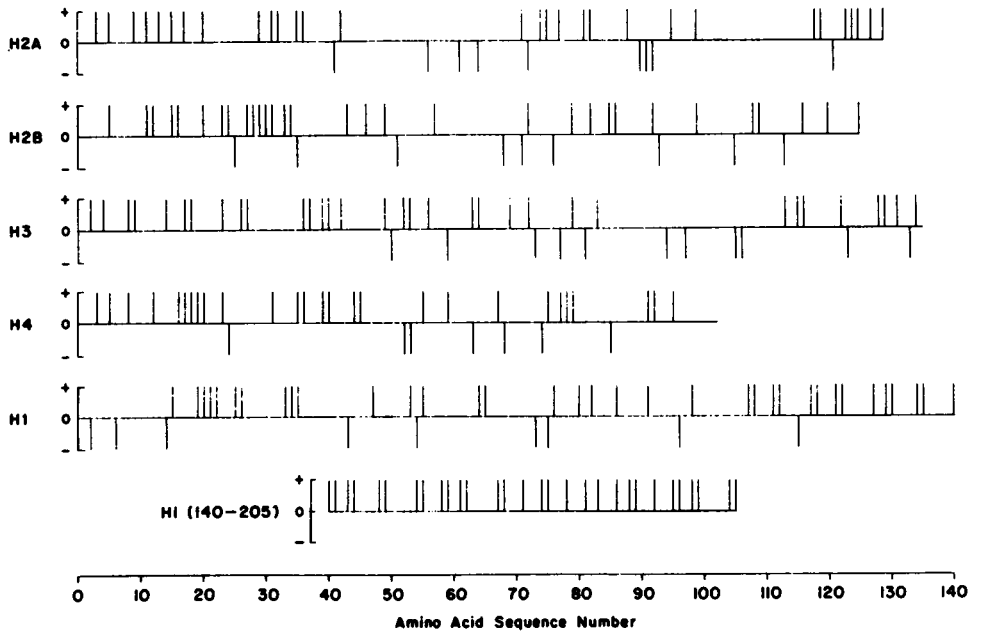

FIGURE 5 The charge distributions of the five histones at pH 7. Upward projecting bars to (+) denote Arg, His, and Lys residues while downward projecting bars to (−) denote Asp and Glu residues.

From a statistical analysis (Palau and Puigdomenech, 1974) of proteins and a stereochemical theory (Lim, 1974) of globular protein secondary structure it has been shown that hydrophobic triplets occupying positions 1-2-5 and 1-4-5 favor helix stabilization. On the other hand, Lewis and Bradbury (1974) found that the attractive and repulsive electrostatic interactions of the i^{th} residue with its neighbors $i \pm 1, 2, 3, 4$, and 7 to be helix-breaking if there is more than one net repulsion. Furthermore, Maxfield and Scheraga (1975) reported helix-disruptive effects of some charged residues at the $i \pm 4$ positions, whereas helix-stabilizing effects were found with oppositely charged residues at the $i \pm 2$ and $i \pm 3$ positions. If electrostatic interactions are taken into consideration, so that charge repulsion between residues will be helix breaking, especially at the $i \pm 3$ and $i \pm 4$ positions, the predicted helicity of H1 is drastically reduced from 55% to 16% (Table III).

H1: Physical-Chemical Studies; Correlation with Predicted Structure; Optical Rotatory Dispersion (ORD), Circular Dichroism (CD) and Nuclear Magnetic Resonance (NMR) Studies

Optical rotatory dispersion (ORD) studies on H1 indicated essentially a random coil structure in aqueous media (Tuan and Bonner, 1969). Upon addition of salt the α-helical content increased to $\simeq$30%. The study of Tuan and Bonner (1969) concluded that the conformation of H1 and other individual histones was ionic strength depend-

TABLE III

THE MAXIMUM AND MINIMUM PERCENT α-HELIX AND PERCENT β-SHEET PREDICTED FOR THE HISTONES BASED ON ELECTROSTATIC INTERACTIONS AND α→β TRANSITIONS

Histone	Percent α		Percent β	
	Max.*	Min.†	Max.§	Min.*
H1	55	16 (16) ‖	5	5
H2A	40	22 (5) ‖	34	19
H2B	35	21 (13) ‖	27	20
H3	39	16 (12) ‖	25	15
H4	28	11 (0) ‖	37	31

*The maximum percent α and minimum percent β are calculated from the predicted α- and β-regions shown in the schematic diagrams of the five histones.

†The minimum percent α is calculated from the predicted stable helices which are unaffected by charge repulsion.

§The maximum percent β is calculated from the predicted β-regions plus new β-regions arising from α → β transitions listed in Table V.

‖ The absolute minimum percent α shown in parenthesis is calculated from the predicted stable helices unaffected by charge repulsion or α → β transition.

ent and changed on association with DNA. In organic solvents a maximum helical content of ≃50% was found (Jirgensons and Hnilica, 1965).

Recent, more exacting CD studies have shown that a small amount of structure exists even at low ionic strength, 3% α and 7% β (Table IV); in 0.14 M NaF the conformation changed to 4% α and 13% β. The phosphorylation of H1 (one or two residues) did not alter its CD spectrum (Adler et al., 1971; Adler et al., 1972), although this modification greatly altered its binding to DNA, as did maleylation (Burnotte et al., 1973). The binding of H1 to DNA caused changes in its conformation, which were difficult to analyze (Tuan and Bonner, 1969; Fasman et al., 1971; Adler and Fasman, 1971).

The NMR studies of Bradbury and colleagues (Bradbury, Cary, Chapman, et al., 1975; Boublik et al., 1970, 1971; Bradbury and Rattle, 1972; Bradbury, Carpenter, and Rattle, 1973), in agreement with the optical rotatory studies, indicate that a change of conformation to a more structured organization occurs upon the addition of salt to H1. These authors conclude that the ordered region occurs between residues (40–115) (Bradbury, Cary, Chapman, et al., 1975) (Table V).

The NMR data suggested that 37% of the structure (40–115) was immobilized in ordered regions (Bradbury, Cary, Chapman, et al., 1975, and the CD studies indicated only 17% structure (4% α, 13% β) (Adler, unpublished). In contrast, the maximal predicted structure contained 55% α, 5% β, and 24% β-turns, a total of 84% ordered structure. However, the predicted conformation is the *maximal* possible ordered structure for the sequence of H1, which is obviously not that found under the conditions reported for the CD measurements (0.14 M NaF). In 1.0 M NaCl a higher helical content of 15% was reported (Bradbury, Cary, Chapman, et al., 1975). The minimal

TABLE IV

SECONDARY CONFORMATION OF HISTONES DETERMINED BY CD DATA

Histone	Low ionic strength*		Solvent	Ref.**	High ionic strength*		Solvent	Ref.**	High ionic strength†§			Solvent	Ref.**
									Fast step	Slow step ‖			
	Percent α	Percent β			Percent α	Percent β			Percent α	Percent α	Percent β		
H1	3	7	0.01 M NaF	a	4	13	0.14 M NaF	e	—	—	—	—	—
H2A	8	26	H_2O	b	15	31	0.14 M NaF	b	14	None		Na_2HPO_4§	f
H2B	10	29	0.01 M NaF	c	14	29	0.14 M NaF	c	14	None		Na_2HPO_4§	g
H3 SH	4	39	H_2O	b	9	39	0.14 M NaF	b	14	8	24	Na_2HPO_4§	h
SS	11	29	H_2O	b	15	31	0.14 M NaF	b	—	—	—	—	—
H4	7	38	5×10^{-3} M NaF	d	19	30	0.14 M NaF	d	15	15	32	Na_2HPO_4§	i

*Using CD standards of Greenfield and Fasman (1969). When Chen et al. (1972) standards are used percent α reduces by 3% and percent β by 13%.

†Standard solvent for random coil: H3 = 10^{-3} M HCl + 10^{-4} M DTT; H2A = 10^{-4} M HCl, others H_2O: α-helix and β reference spectra. Greenfield and Fasman (1969).

§Sodium phosphate, pH 7.0, concentration < 0.03 M, various times. See references.

‖ Values after completion of both fast and slow step.

**References: (a) Adler, unpublished; (b) Adler, Moran, and Fasman, 1975; (c) Adler, Ross, et al., 1974; (d) Adler, Fulmer, and Fasman, 1975; (e) Fasman et al., 1970; (f) D'Anna and Isenberg, 1974*b*; (g) D'Anna and Isenberg, 1972; (h) D'Anna and Isenberg, 1974*a*; (i) Wickett et al., 1972.

TABLE V

STRUCTURED HISTONE REGIONS BASED ON NMR DATA

Histone	Structured portion	Ref.
H1	40–115	Bradbury, Cary, Chapman et al. (1975)
H2A	25–113	Bradbury, Cary, Crane-Robinson et al. (1975)
H2B	31–102	Bradbury, Cary et al. (1972)
H3	42–110	Bradbury, Cary et al. (1973)
H4	33–102	Bradbury and Rattle (1972)
	≈ (70–80)–102	Pekary et al. (1975*b*)
	25–67 (Nucleus for structure)	Lewis et al. (1975)

predicted structure (Table III) contains 16% α and 5% β which agrees well with this CD estimate. In the region (40–115, 76 residues), which NMR studies (Bradbury, Cary, Chapman, et al., 1975) show to be structured, there are three-α-helices predicted (38 residues), two β-sheet regions (10 residues), and six β-turns (20 residues), a total of 68 residues. Thus there is 94% (72 residues out of a possible 75 residues) agreement between NMR and the present prediction for this region. However, outside the NMR structured region there are nine other α-regions and nine β-turns predicted. Thus in the most propitious environment H1 is capable of assuming a more ordered structure than found in the NMR or CD studies.

It is interesting to note (Fig. 4) that the stable helices (41–55) and (60–69) and the anti-parallel β-sheets (85–97) are located within the structured region (40–115) determined from NMR (Bradbury, Cary, Chapman, et al., 1975). Furthermore, the 22% helix and 6% β-sheet found, in 1.5 M NaCl, for the N-terminal fragment (1-106) of H1 from CD analysis (Bradbury, Chapman, et al., 1975) agree well with the predicted 24% α and 9% β in this N-segment. Similarly, the 6% α and 0% β found in the C-terminal fragment (107–205) of H1 from CD studies (Bradbury, Chapman, et al., 1975) correlate well with the 7% α-helix (149–155) and 0% β from prediction of stabilized regions in this C-segment.

In the present discussion β-turns have been included in the ordered secondary structures. In the X-ray determination of protein structure the β-turns were most frequently ignored, however, in the analysis of these structures (Chou and Fasman, 1974*a*,*b*) it was found that $\simeq$29% of the amino acids in globular proteins were involved in β-turns. Since β-turns play an important role in secondary structure, as they are highly ordered and make the initial folds for tertiary structure, they should unequivocally be counted into the secondary structure of proteins.

H2A: Prediction of the Secondary Structure

The sequence of histone H2A is given in Fig. 6 (Yoeman et al., 1972; Sautiere et al., 1974). Applying the conformational parameters from 29 proteins and the rules previously formulated (Chou and Fasman, 1974*a*, *b*), the conformational profile of the α-helical and β-sheet regions can be obtained and is seen in Fig. 7. The predicted α-helix, β-sheet, and coil regions for H2A are given in Table VI. The relative com-

H2A : CALF THYMUS

129 AMINO ACID RESIDUES

1	2	3	4	5	6	7	8	9	10	11	12	13	14	15
SER-	GLY-	ARG-	GLY-	LYS-	GLN-	GLY-	GLY-	LYS-	ALA-	ARG-	ALA-	LYS-	ALA-	LYS-
16	17	18	19	20	21	22	23	24	25	26	27	28	29	30
THR-	ARG-	SER-	SER-	ARG-	ALA-	GLY-	LEU-	GLN-	PHE-	PRO-	VAL-	GLY-	ARG-	VAL-
31	32	33	34	35	36	37	38	39	40	41	42	43	44	45
HIS-	ARG-	LEU-	LEU-	ARG-	LYS-	GLY-	ASN-	TYR-	ALA-	GLU-	ARG-	VAL-	GLY-	ALA-
46	47	48	49	50	51	52	53	54	55	56	57	58	59	60
GLY-	ALA-	PRO-	VAL-	TYR-	LEU-	ALA-	ALA-	VAL-	LEU-	GLU-	TYR-	LEU-	THR-	ALA-
61	62	63	64	65	66	67	68	69	70	71	72	73	74	75
GLU-	ILE-	LEU-	GLU-	LEU-	ALA-	GLY-	ASN-	ALA-	ALA-	ARG-	ASP-	ASN-	LYS-	LYS-
76	77	78	79	80	81	82	83	84	85	86	87	88	89	90
THR-	ARG-	ILE-	ILE-	PRO-	ARG-	HIS-	LEU-	GLN-	LEU-	ALA-	ILE-	ARG-	ASN-	ASP-
91	92	93	94	95	96	97	98	99	100	101	102	103	104	105
GLU-	GLU-	LEU-	ASN-	LYS-	LEU-	LEU-	GLY-	LYS-	VAL-	THR-	ILE-	ALA-	GLN-	GLY-
106	107	108	109	110	111	112	113	114	115	116	117	118	119	120
GLY-	VAL-	LEU-	PRO-	ASN-	ILE-	GLN-	ALA-	VAL-	LEU-	LEU-	PRO-	LYS-	LYS-	THR-
121	122	123	124	125	126	127	128	129						
GLU-	SER-	HIS-	HIS-	LYS-	ALA-	LYS-	GLY-	LYS-						

FIGURE 6 The amino acid sequence of histone H2A (calf thymus). As determined by Yeoman et al. (1972) and Sautiere et al. (1974).

position of the various conformational regions are: α-helix, 40%; β-sheet, 20%; and random coil, and/or β-turns 40%. There are five helical regions, composed of 52 residues; five β-sheet regions, composed of 25 residues; and the remaining 52 amino acids having the random or β-turn conformation. The relative probability that a tetrapeptide will form a β-turn is depicted in the probability profile shown in Fig. 8. The result of the β-turn prediction is summarized in Table VI, showing the 10 specific β-turns, which is 30% of the sequence. Only 10% of the sequence is predicted to be in unstructured regions.

The summation of the predicted secondary structure of H2A is represented in the schematic diagram, Fig. 9. As depicted, there are two regions where internal antiparallel β-sheet association is a possibility: one at (23–27) to (30–34), with a β-turn at (27–30) and the other at (76–79) to (100–104). A β-turn (88–91) may also exist between the two helices (81–88) and (91–97). However, these tertiary structure projections are entirely speculative.

The uneven distribution of the amino acid residues, the charged groups and hydro-

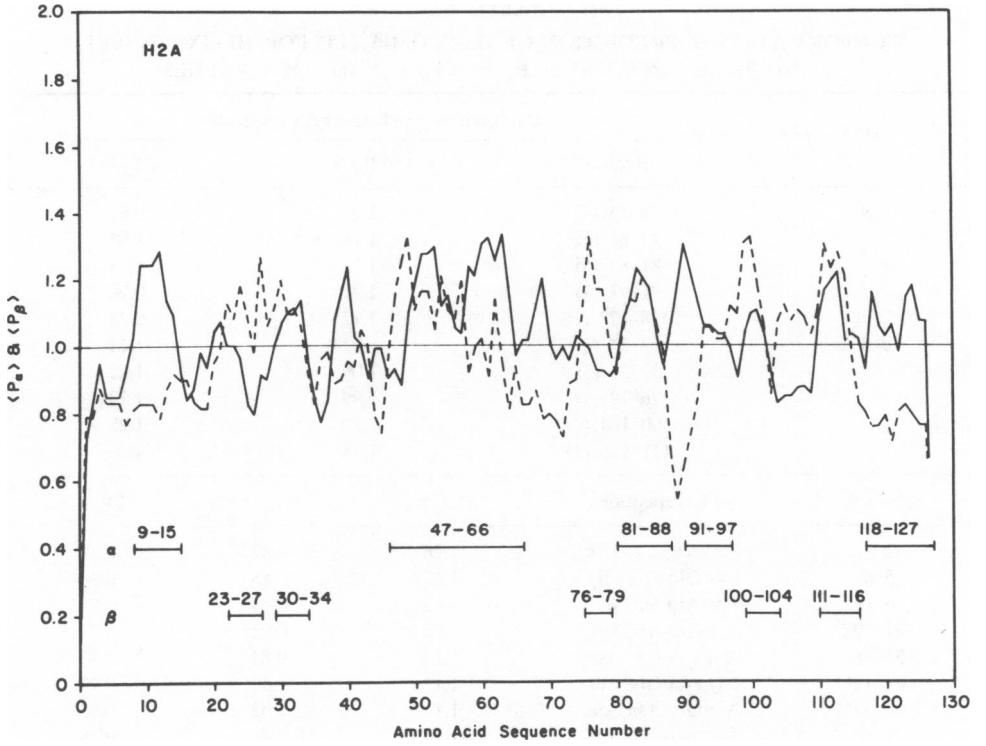

FIGURE 7 The conformational profile of H2A. (——), helical potential $<P\alpha>$ of tetrapeptide i to i + 3. (- - - -), β-sheet potential $<P_\beta>$ of tetrapeptide i to i + 3. Regions with helical and β-sheet-forming potential lie above the cut-off point 1.0 with tetrapeptide breakers falling below 1.0. The predicted α- and β-regions are underlined.

phobic regions, are shown in Fig. 5. It can be seen that in H2A the basic residues are clustered between residues (1–36) and between (118–129) (Fig. 9). However, in the schematic representation there are two α-helical regions predicted which have similar high charge [(9–15) and (118–127)]; these helices should be unfavorable due to charge repulsion. For the reasons discussed above (for H1) the prediction for H2A is the *maximal* potential found for the various conformations, and may occur when the histones are found under the proper environmental conditions (also discussed above).

When charge repulsion is taken into consideration a minimum secondary structure is calculated to contain 22% α and 19% β (Table III). Regions of H2A capable of undergoing conformational changes due to environmental conditions are shown in Table VII. The long helical section (47–66) could form two β-sections, (49–55) and (57–63) whose $<P_\beta> > <P_\alpha>$. The strong β-breaker Glu 56 prevents the formation of a long β-segment. There is another possibility of an $\alpha \rightarrow \beta$ change at (83–87). While these three newly formed β-regions do not appear to interact with the existing β-regions predicted for H2A, they may be involved in association sites with other histone complexes.

TABLE VI

CONFORMATIONAL PREDICTION OF H2A COMPUTED FOR HELIX, β-SHEET, AND β-TURN REGIONS: $<P_\alpha>$, $<P_\beta>$, AND $<P_t>$ VALUES

H2A	Calf thymus (prediction) 129 residues		
	Region*	$<P_\alpha>$†	$<P_\beta>$†
Helix	9–15 (7)	1.25	0.81
	47–66 (20)	1.18	1.07
	81–88 (8)	1.12	1.11
	91–97 (7)	1.21	0.90
	118–127 (10)	1.12	0.78
β-sheet	23–27 (5)	1.02	1.21
	30–34 (5)	1.09	1.22
	76–79 (4)	0.99	1.33
	100–104 (5)	1.10	1.28
	111–116 (6)	1.18	1.30

β-turn§	Tetrapeptide	$<P_t>$†	$<P_\alpha>$†	$<P_\beta>$†
2–5	Gly-Arg-Gly-Lys	1.26	0.82	0.79
5–8	Lys-Gln-Gly-Gly	1.27	0.85	0.84
16–19	Thr-Arg-Ser-Ser	1.19	0.84	0.91
27–30‖	Val-Gly-Arg-Val	0.88	0.92	1.27
35–38	Arg-Lys-Gly-Asn	1.27	0.84	0.83
44–47**	Gly-Ala-Gly-Ala	1.11	1.00	0.79
66–69**	Ala-Gly-Asn-Ala	1.11	1.02	0.83
71–74	Arg-Asp-Asn-Lys	1.24	0.96	0.78
73–76	Asn-Lys-Lys-Thr	1.13	0.96	0.89
88–91**	Arg-Asn-Asp-Glu	1.18	1.04	0.68
108–111	Leu-Pro-Asn-Ile	1.03	0.88	1.09

Helix: 40%	β-turns: 30%
β-sheet: 20%	Coil: 10%

*†See footnotes in Table I.

§Based on probability profile of Fig. 8.

‖ Although the β-turn probability (Fig. 8) at 26–29 is higher ($p_t = 7.9 \times 10^{-5}$) with $<P_t> = 1.13 > <P_\beta> = 0.98 > <P_\alpha> = 0.80$, the β-turn was chosen as 27–30 allowing better anti-parallel β-sheet juxtaposition between regions 23–27 and 30–34.

**β-turns are predicted at positions 44–47, 66–69, and 88–91 from their $<P_t>$ values even though their p_t values were slightly above average ($<p_t> = 5 \times 10^{-5}$).

H2A: Physical-Chemical Studies; Correlation with Predicted Structure; ORD, CD, NMR

Early ORD studies (Bradbury et al., 1967) on H2A indicated a random conformation in aqueous media, with increasing helicity in higher ionic strength solutions (18% α, in 0.5 M NaCl), while in 2-chloroethanol a maximum helical content of 65% was observed. Recent CD studies (Bradbury, Cary, Crane-Robinson, et al., 1975; Adler, Moran, and Fasman, 1975; D'Anna and Isenberg, 1974*a*) have demonstrated a zero or very low helix content (8%) in aqueous medium (see Table IV), with a β content of

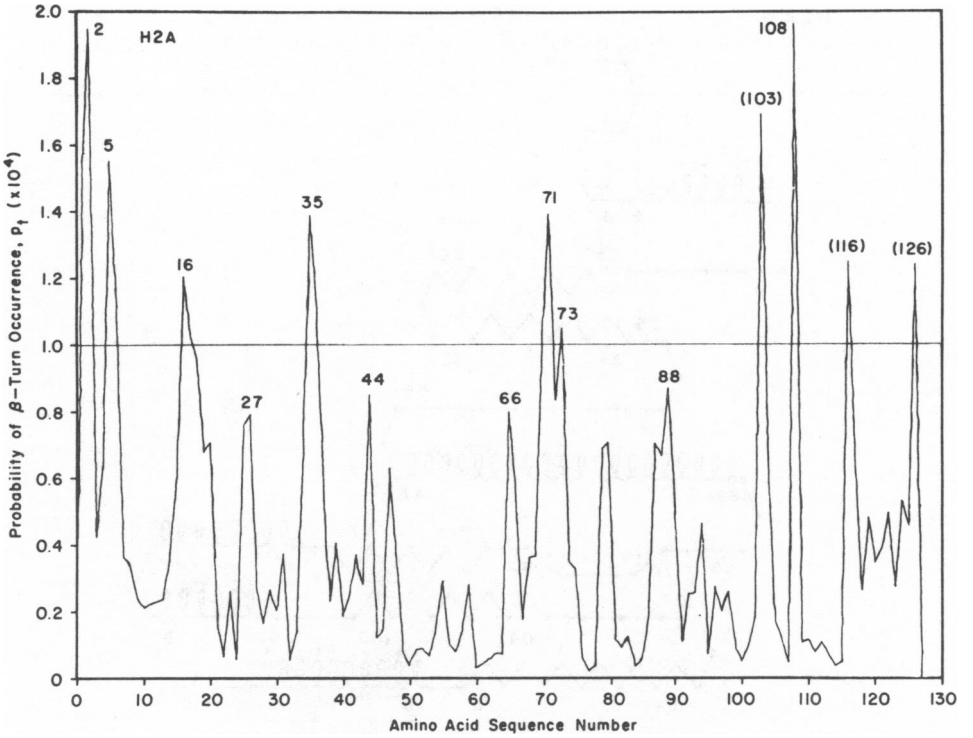

FIGURE 8 Probability of tetrapeptide β-turns in H2A. The horizontal line corresponds to an arbitrary cut-off value of 1.0×10^{-4}. Of the 10 sharp peaks above the cut-off, 7 were predicted as β-turns, while 3 were excluded (residue number shown in parentheses) as belonging to other regions. Four peaks below the cut-off were predicted as β-turns for reasons given in Table VI.

26% (Adler, Moran, and Fasman, 1975), while at higher ionic strength, helical contents between 14 and 28%, with 0–31% β structure were found.

D'Anna and Isenberg (1974*b*) have shown that H2A undergoes a conformational change in the presence of salts: phosphate was especially effective (Table IV). An instantaneous change upon addition of phosphate produced a 14% helical content. These results for the α content are in agreement with Adler et al. (1975) who also estimate a 31% β content. There are other reports of high helical content at high salt concentrations (28% α, 36 residues in 2.00 M NaCl [Bradbury, Cary, Crane-Robinson, et al., 1975], and 23% α and 18% β in 1 M KF or 10^{-1} M PO_4 [Garel et al., 1975*a*]). The differences in evaluation are strongly dependent on the standards used.

NMR studies have also shown the ionic strength dependence of structured regions (Bradbury, Cary, Crane-Robinson, et al., 1975; Clark et al., 1974). Residues (25–113) were estimated to be involved in structured regions, with the end regions remaining free (Bradbury, Cary, Crane-Robinson, et al., 1975) (Table V). Upon addition of H2A to DNA, the amino and carboxyl termini become restricted.

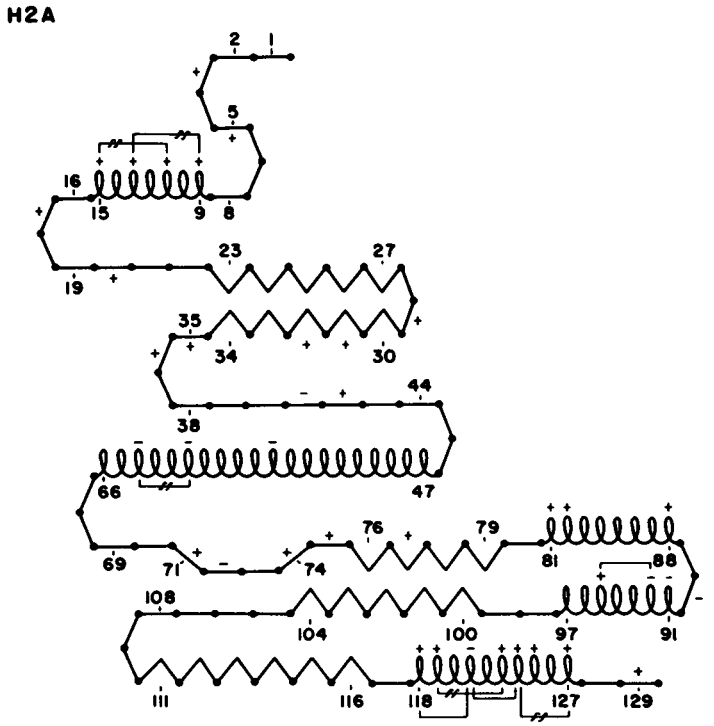

FIGURE 9 Schematic diagram of the secondary structure predicted for H2A. Residues are represented in helical (ℓ), β-sheet ($\wedge$), and coil (——) conformational states. Chain reversals indicate β-turn tetrapeptides. Helices with (⌐§§¬) contain charge repulsion between $i \pm 3$ or $i \pm 4$ residues and will be disrupted at low ionic strength, but may be stabilized at high ionic strength or upon interaction with DNA phosphates.

When H2A interacted with DNA a conformational change in the histone was observed (e.g., Garel et al., 1975*b*), and this was attributed to changes in mobility of the two basic ends of the molecule (Bradbury, Cary, Crane-Robinson, et al., 1975).

The NMR data (Bradbury, Cary, Crane-Robinson, et al., 1975) suggests a 68% ordered structure and the prediction for this "NMR-structured" region (25–113, 89 residues) contains 64% of the whole molecule (three α-helices, 35 residues; five β-sheets, 25 residues, and seven β-turns, 21 residues: total 81 residues). The CD estimate of structure, in 0.14 M NaF, suggests a much lower ordered structure, 46% (15% α, 31% β), while in 2.0 M NaCl, a 28% α content was found (Bradbury, Cary, Crane-Robinson, et al., 1975). Thus the maximal structured value, estimated by the prediction, is not found under the conditions used for the measurements in solution. Outside the ordered NMR region there are two unstable α-helices and three β-turns predicted.

From the schematic diagram of H2A (Fig. 9) it may be seen that helices (9–15) and (118–127) are easily disrupted by charged repulsion. On the other hand, the predicted stable helices (47–66), (81–88), and (91–97) are all contained in the structured region (25–113) deduced from NMR studies (Bradbury, Cary, Crane-Robinson, et al., 1975).

TABLE VII

REGIONS IN HISTONES WITH POTENTIAL FOR $\alpha \rightarrow \beta$ TRANSITIONS*

	Original values		New region	Potential new values	
	$<P_\alpha>$	$<P_\beta>$		$<P_\alpha>$	$<P_\beta>$
Histone H2A					
47–66 α (20)	1.18	1.07	49–55 β (7)	1.15	1.30
			57–63 β (7)	1.14	1.15
81–88 α (8)	1.12	1.11	83–87 β (5)	1.21	1.23
Original conformation	40% α	19% β			
Net change	−22% α	+14% β			
New conformation	19% α	34% β			
Histone H2B					
93–102 α (10)	1.16	1.16	94–102 β (9)	1.12	1.25
Original conformation	34% α	20% β			
Net change	−8% α	+7% β			
Net conformation	26% α	27% β			
Histone H3					
45–53 α (9)	1.12	1.09	45–48 β (4)	1.13	1.26
67–79 α (13)	1.15	1.07	67–71 β (5)	1.10	1.28
			74–78 β (5)	1.15	1.09
Original conformation:	39% α	15% β			
Net change:	−16% α	+10% β			
New conformation:	23% α	25% β			
Histone H4					
57–67 α (11)	1.10	1.24	57–62 β (6)	1.14	1.35
Original conformation	28% α	31% β			
Net change	−11% α	+6% β			
New conformation	17% α	37% β			
Histone H1					
No $\alpha \rightarrow \beta$ transitional regions predicted					
Original conformation	55% α	5% β			

*The basis for the predicted $\alpha \rightarrow \beta$ transitions lies in the fact that several of the predicted helical regions also have residues with β-sheet-forming potentials. If three β-formers out of five residues are found in these α-regions, that portion of the helix containing the β-formers will undergo an $\alpha \rightarrow \beta$ transformation.

The 22% α for the three stable helices predicted in H2A compares well with the CD estimate of 15% α in 0.14 M NaF (Adler, Moran, and Fasman, 1975), 23% α in 10^{-3} M phosphate (Garel et al., 1975*a*), 19–26% α in 0.10–2.0 M NaCl, and 20–26% α in 0.1–1.0 M phosphate (Bradbury, Cary, Crane-Robinson, et al., 1975). Although Bradbury et al. found no β-structure in H2A from CD and IR analysis, Garel et al. (1975*a*) reported 18% β in 10^{-3} M phosphate buffer which agrees well with the 19% β predicted. It is quite possible that the predicted β-sheets (23–27), (30–34), (76–79), (100–104), and (111–116) as well as the three stable helices in the structured region (25–113) are involved in the intermolecular association of H2A proposed by Bradbury, Cary, Crane-Robinson, et al., (1975). These authors suggested that all three Tyr residues 39, 50, 57, are spatially close together when a two-dimensional helical surface of H2A was constructured. However, Gly 44 and Gly 46 are helix-breaking and the predicted β-turn at (44–47) may bring Tyr 39 further away from Tyr 50 but closer to Tyr 57 (Fig. 9). In ad-

H2B - BOVINE 125 AMINO ACID RESIDUES

1	2	3	4	5	6	7	8	9	10	11	12	13	14	15
PRO-	GLN-	PRO-	ALA-	LYS-	SER-	ALA-	PRO-	ALA-	PRO-	LYS-	LYS-	GLY-	SER-	LYS-
16	17	18	19	20	21	22	23	24	25	26	27	28	29	30
LYS-	ALA-	VAL-	THR-	LYS-	ALA-	GLN-	LYS-	LYS-	ASP-	GLY-	LYS-	LYS-	ARG-	LYS-
31	32	33	34	35	36	37	38	39	40	41	42	43	44	45
ARG-	SER-	ARG-	LYS-	GLU-	SER-	TYR-	SER-	VAL-	TYR-	VAL-	TYR-	LYS-	VAL-	LEU-
46	47	48	49	50	51	52	53	54	55	56	57	58	59	60
LYS-	GLN-	VAL-	HIS-	PRO-	ASP-	THR-	GLY-	ILE-	SER-	SER-	LYS-	ALA-	MET-	GLY-
61	62	63	64	65	66	67	68	69	70	71	72	73	74	75
ILE-	MET-	ASN-	SER-	PHE-	VAL-	ASN-	ASP-	ILE-	PHE-	GLU-	ARG-	ILE-	ALA-	GLY-
76	77	78	79	80	81	82	83	84	85	86	87	88	89	90
GLU-	ALA-	SER-	ARG-	LEU-	ALA-	HIS-	TYR-	ASN-	LYS-	ARG-	SER-	THR-	ILE-	THR-
91	92	93	94	95	96	97	98	99	100	101	102	103	104	105
SER-	ARG-	GLU-	ILE-	GLN-	THR-	ALA-	VAL-	ARG-	LEU-	LEU-	LEU-	PRO-	GLY-	GLU-
106	107	108	109	110	111	112	113	114	115	116	117	118	119	120
LEU-	ALA-	LYS-	HIS-	ALA-	VAL-	SER-	GLU-	GLY-	THR-	LYS-	ALA-	VAL-	THR-	LYS-
121	122	123	124	125										
TYR-	THR-	SER-	SER-	LYS-										

FIGURE 10 The amino acid sequence of histone H2B (bovine). As determined by Iwai et al. (1970).

dition the proximity of Phe 25 and His 31 may not be due to the helical model (Bradbury, Cary, Crane-Robinson, et al., 1975) but instead due to the anti-parallel β-sheets (23–27) and (30–34). The broadening of the Phe 25 and His 31 resonances detected by NMR may be interpreted as β:β intermolecular interactions rather than α:α association.

H2B: Prediction of Secondary Structure

The sequence of histone H2B is given in Fig. 10 (Iwai et al., 1970). The application of the prediction technique (Chou and Fasman, 1974a, *b*) produces the conformational profile for the α-helical and β-sheet regions, which is seen in Fig. 11. These predicted sections are summarized in Table VIII. The secondary composition of H2B is: 35% α, 20% β, and 45% random coil and/or β-turns. There are four helical sections, composed of 43 residues, four β-sheet regions, consisting of 25 residues and 56 residues in β-turns or the disordered conformation. The probability profile of tetrapeptide β-turns is depicted in Fig. 12, and is summarized in Table VIII. The eight β-turns are well distributed throughout the molecule, containing 26% of the residues in the molecule. The random structure is made of 19% of the residues. The overall predicted secondary structure of H2B is schematically presented in Fig. 13.

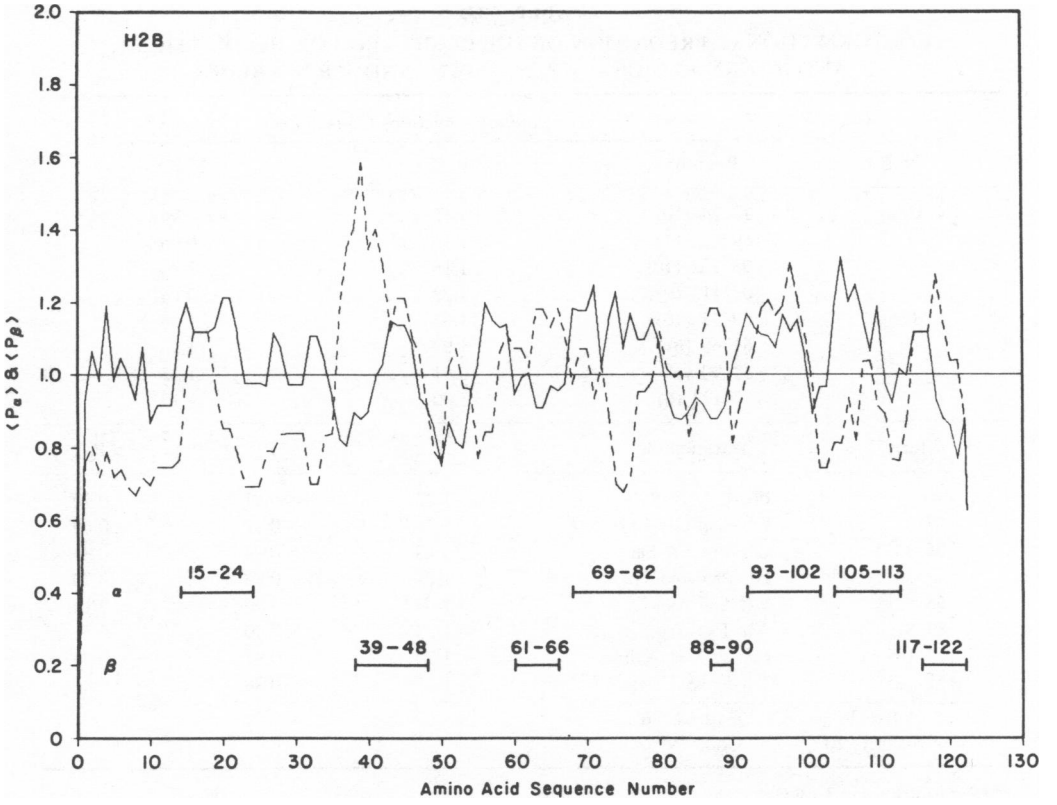

FIGURE 11 The conformational profile of H2B. (——), helical potential $<P_\alpha>$ of tetrapeptide i to i + 3. (- - - -), β-sheet potential $<P_\beta>$ of tetrapeptide i to i + 3. Regions with helical and β-forming potential lie above the cut-off point 1.0 with tetrapeptide breakers falling below 1.0. The predicted α- and β-regions are underlined.

The uneven distribution of charges in H2B is seen in Fig. 5. There is a concentration of positive charge in the NH_2-terminus (1–35). When these charge repulsions are considered, the predicted structure reduces to 21% α and 20% β (Table III), leaving the stable helices (76–82), (93–102), and (105–113).

An $\alpha \rightarrow \beta$ transition at (93–102) is possible (Table VII) since the α and β-potentials are identical ($P_\alpha = P_\beta = 1.16$). This region was predicted to be helical rather than β since there are five strong helix formers and only two strong β-formers. The newly formed β-sheet (94–102) will lack the strong β-breaker Glu 93.

H2B: Physical-Chemical Studies; Correlation with Predicted Structure; ORD, CD, NMR

ORD studies have indicated that H2B has a random conformation in aqueous media (e.g., Bradbury et al., 1972), and the helical content increases to $\simeq$30% in 1.0 M NaCl. Recent CD studies have indicated that H2B is not totally random at low ionic strength

TABLE VIII

CONFORMATIONAL PREDICTION OF H2B COMPUTED FOR HELIX, β-SHEET, AND β-TURN REGIONS: $<P_\alpha>$, $<P_\beta>$, AND $<P_t>$ VALUES

	Bovine (prediction) 125 residues		
H2B	Region*	$<P_\alpha>$†	$<P_\beta>$†
Helix	15–24 (10)	1.16	0.94
	69–82 (14)	1.15	0.96
	93–102 (10)	1.16	1.16§
	105–113 (9)	1.23	0.86
β-sheet	39–48 (10)	1.03	1.36
	61–66 (6)	1.03	1.23
	88–90 (3)	0.91	1.33
	117–122 (6)	1.00	1.19

β-turn‖	Tetrapeptide	$<P_t>$†	$<P_\alpha>$†	$<P_\beta>$†
10–13	Pro-Lys-Lys-Gly	1.27	0.87	0.70
24–27	Lys-Asp-Gly-Lys	1.26	0.98	0.69
35–38**	Glu-Ser-Tyr-Ser	1.19	0.94	0.84
49–52	His-Pro-Asp-Thr	1.22	0.85	0.79
66–69††	Val-Asn-Asp-Ile	1.00	0.96	1.18
84–87	Asn-Lys-Arg-Ser	1.23	0.90	0.83
102–105	Leu-Pro-Gly-Glu	1.10	0.97	0.74
122–125	Thr-Ser-Ser-Lys	1.21	0.88	0.86

Helix: 35%	β-turns: 26%
β-sheet: 20%	Coil: 19%

*†See footnotes in Table I.

§This region is predicted as helical from hierarchical analysis (Chou and Fasman, 1974*b*) showing $(H_5h_3i_2)_\alpha$ and $(H_2h_5i_2B)_\beta$ although their $<P_\alpha>$ and $<P_\beta>$ are identical.

**Predicted as β-turn since $<P_t> = 1.19 > <P_\alpha>$ and $<P_\beta>$.

††Although no tetrapeptide between residues 51 and 82 has a high probability of β-turn occurrence (see Fig. 12), tetrapeptide 66–69 was selected as a β-turn to allow chain reversal in this region, permitting possible stabilization of β-sheet 61–66 with helix 69–82.

(0.01 M NaF, 10% α, 29% β) (Table IV), and in 0.14 M NaF becomes slightly more helical (14% α, 29% β) (Adler et al., 1974*a*). In the presence of phosphate a fast conformational change occurs yielding 14% α-helix (D'Anna and Isenberg, 1972, 1973). NMR studies have shown that the molecule has restricted rotational freedom in the (31–102) region (Table III), when the ionic strength is raised (Boublik et al., 1971).

The conformation of H2B is changed upon binding DNA (Adler, Fasman, et al., 1974) and NMR studies indicate that regions (1–30) and (102–125) are involved in the binding (Boublik et al., 1971).

The NMR data (Bradbury et al., 1972) suggests an ordered region (31–102) comprising 65% of the molecule. Within this region the prediction has two α-helices (25 residues), three β-sheets (19 residues), and five β-turns (16 residues), giving an 83% ordered structure (60 residues). The remaining residues could easily be immobilized by the presence of the ordered regions. Beyond the NMR-detected ordered section,

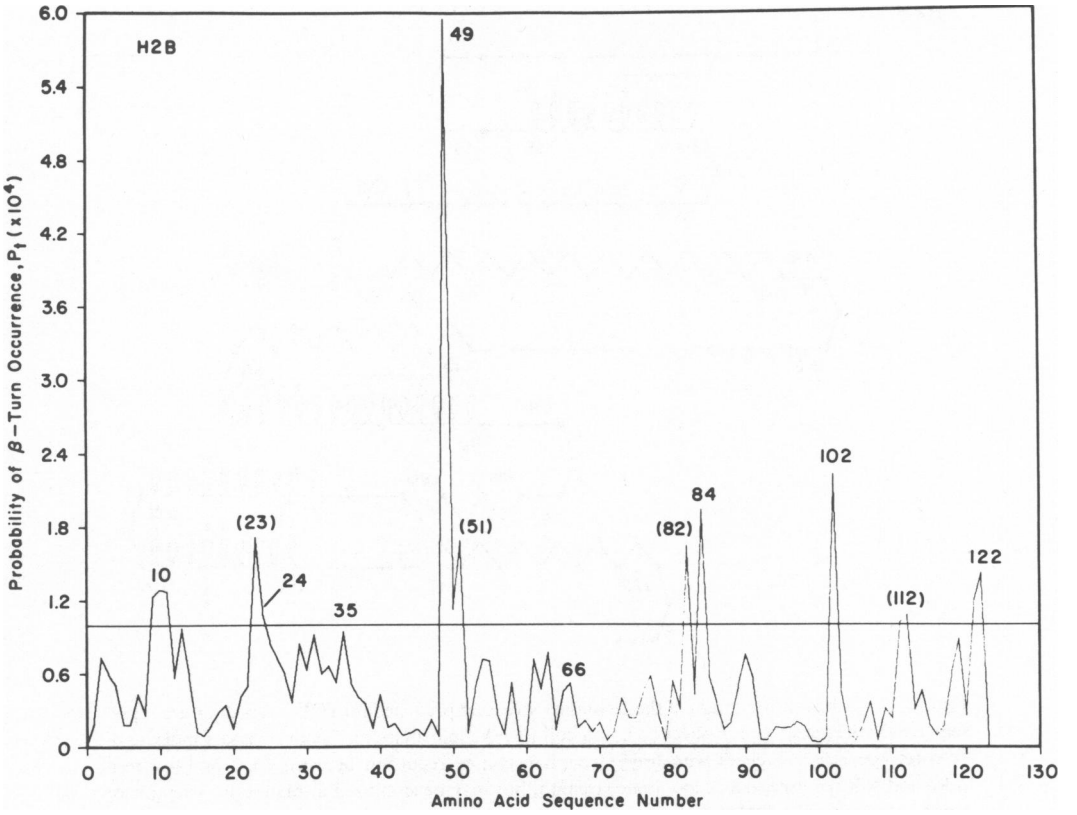

FIGURE 12 Probability of tetrapeptide β-turns in H2B. The horizontal line corresponds to an arbitrary cut-off value of 1.0×10^{-4}. Of the 10 sharp peaks above the cut-off, 6 were predicted as β-turns, while 4 were excluded (residue number shown in parentheses) as belonging to other regions. Two peaks below the cut-off were also predicted as β-turns for reasons given in Table VIII.

the prediction places two α-helices, one β-sheet, and three β-turns, accounting for the remaining 35% structure.

The predicted stable helices in H2B (Fig. 13), unaffected by charge repulsion, are (76–82), (93–102), and (105–113) amounting to 21% α (Table III). This value lies within the range of 14% α–26% α (at pH 7.4 and pH 3.5) obtained in high salt from the CD studies (D'Anna and Isenberg, 1972). From NMR spectral changes, Bradbury et al., (1972) suggested that regions (1–30) and (102–125) of H2B interact with DNA while the structured region (31–102) participates in histone-histone interactions. It was also found that the amino half of H2B (1–58) was highly insensitive to salt addition in sharp contrast to the carboxyl half (63–125) which tends to precipitate beyond 0.7 M NaCl (Bradbury and Rattle, 1972). As can be seen from the schematic diagram of H2B (Fig. 13), three helices and three β-sheets are located in the carboxyl half as compared with only one helix and one β-region in the amino half. Hence the more

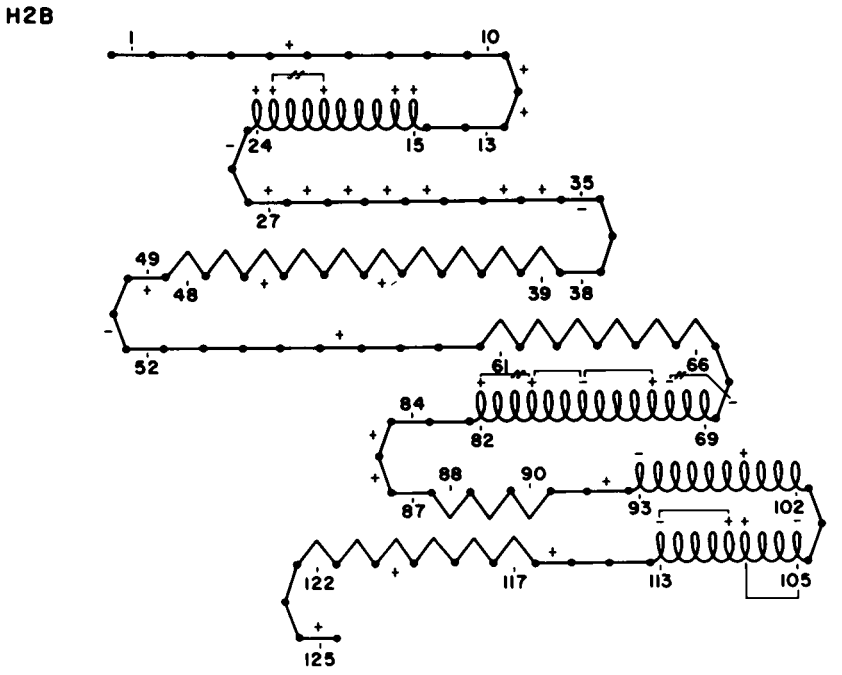

FIGURE 13 Schematic diagram of the secondary structure predicted for H2B. Residues are represented as in the helical (ℓ), β-sheet (∧), and coil (——) conformation. Chain reversals indicate β-turn tetrapeptides. Helices with (⌐§§¬) contain charge repulsion between i ± 3 or i ± 4 residues and will be disrupted at low ionic strength, but may be stabilized at high ionic strength or upon interaction with DNA phosphates.

structured C-terminal half shows much greater sensitivity to salt effects. Furthermore, the spectral broadening of Tyr 37, 40, and 42 as well as His 49 in H2B was interpreted as showing that region (30–50) was involved in interchain interactions (Bradbury et al., 1972). Some form of β:β interaction may be expected since region (39–48) was predicted as a β-sheet. The predicted percent β in H2B ranges from a minimum of 20% to a maximum of 27% (Table III) which compares favorably with 29% β from CD studies (Table VI).

H3: Prediction of Secondary Structure

The sequence of H3 is shown in Fig. 14 (DeLange et al., 1972). The conformational prediction profile of the α-helical and β-regions is shown in Fig. 15. These regions are summarized in Table IX. The molecule is composed of: 39% α, 15% β-sheet, and 46% of β-turns and/or disordered sections. The five helical regions contain 43 residues, the four β-sheet sections contain 20 residues, and the remaining 62 residues are in the random or β-turn conformation. The β-turn probability profile is displayed in Fig. 16 and is summarized in Table IX, showing the eight specific β-turns, comprising 24% of the molecule. The predicted unstructured regions contain 22% of the residues.

The overall maximum predicted secondary structure is displayed in the schematic

H3 CALF THYMUS 135 AMINO ACID RESIDUES

1	2	3	4	5	6	7	8	9	10	11	12	13	14	15
ALA-	ARG-	THR-	LYS-	GLN-	THR-	ALA-	ARG-	LYS-	SER-	THR-	GLY-	GLY-	LYS-	ALA-
16	17	18	19	20	21	22	23	24	25	26	27	28	29	30
PRO-	ARG-	LYS-	GLN-	LEU-	ALA-	THR-	LYS-	ALA-	ALA-	ARG-	LYS-	SER-	ALA-	PRO-
31	32	33	34	35	36	37	38	39	40	41	42	43	44	45
ALA-	THR-	GLY-	GLY-	VAL-	LYS-	LYS-	PRO-	HIS-	ARG-	TYR-	ARG-	PRO-	GLY-	THR-
46	47	48	49	50	51	52	53	54	55	56	57	58	59	60
VAL-	ALA-	LEU-	ARG-	GLU-	ILE-	ARG-	ARG-	TYR-	GLN-	LYS-	SER-	THR-	GLU-	LEU-
61	62	63	64	65	66	67	68	69	70	71	72	73	74	75
LEU-	ILE-	ARG-	LYS-	LEU-	PRO-	PHE-	GLN-	ARG-	LEU-	VAL-	ARG-	GLU-	ILE-	ALA-
76	77	78	79	80	81	82	83	84	85	86	87	88	89	90
GLN-	ASP-	PHE-	LYS-	THR-	ASP-	LEU-	ARG-	PHE-	GLN-	SER-	SER-	ALA-	VAL-	MET-
91	92	93	94	95	96	97	98	99	100	101	102	103	104	105
ALA-	LEU-	GLN-	GLU-	ALA-	CYS-	GLU-	ALA-	TYR-	LEU-	VAL-	GLY-	LEU-	PHE-	GLU-
106	107	108	109	110	111	112	113	114	115	116	117	118	119	120
ASP-	THR-	ASN-	LEU-	CYS-	ALA-	ILE-	HIS-	ALA-	LYS-	ARG-	VAL-	THR-	ILE-	MET-
121	122	123	124	125	126	127	128	129	130	131	132	133	134	135
PRO-	LYS-	ASP-	ILE-	GLN-	LEU-	ALA-	ARG-	ARG-	ILE-	ARG-	GLY-	GLU-	ARG-	ALA-

FIGURE 14 The amino acid sequence of histone H3 (calf thymus). As determined from DeLange et al. (1972).

diagram, Fig. 17. The β-turn (106–109) may form anti-parallel β-sheets between (99–104) and (109–113), while the β-turn (121–124) will stabilize the two β-sheet sections (117–120) and (124–128). The charge distribution of H3 is seen in Fig. 5. The predicted stable helices in H3, unaffected by electrostatic repulsion are (45–50), (58–65), and (88–95), comprising 16% α-helix for the minimum secondary structure (Table III).

The potential conformational changes are listed in Table VII. Two new β-regions can form at (45–48) and (67–71) with $<P_\beta> > <P_\alpha>$. Another segment (74–78), containing 3/5 of β formers is also potentially capable of an $\alpha \rightarrow \beta$ transformation, despite $<P_\alpha> = 1.15 > <P_\beta> = 1.09$. The predicted 15% β in H3 may increase to 25% β due to these α–β transitions (Table VII) and reduce the helicity to 12%.

H3: Physical-Chemical Studies; Correlation with Predicted Structure; ORD, CD, NMR.

The original ORD studies on H3 indicated a random structure in aqueous media (Oh, 1970) which could be altered to a partial helical structure in the presence of salt (1.0 M NaCl, 26% α) (Bradbury et al., 1965).

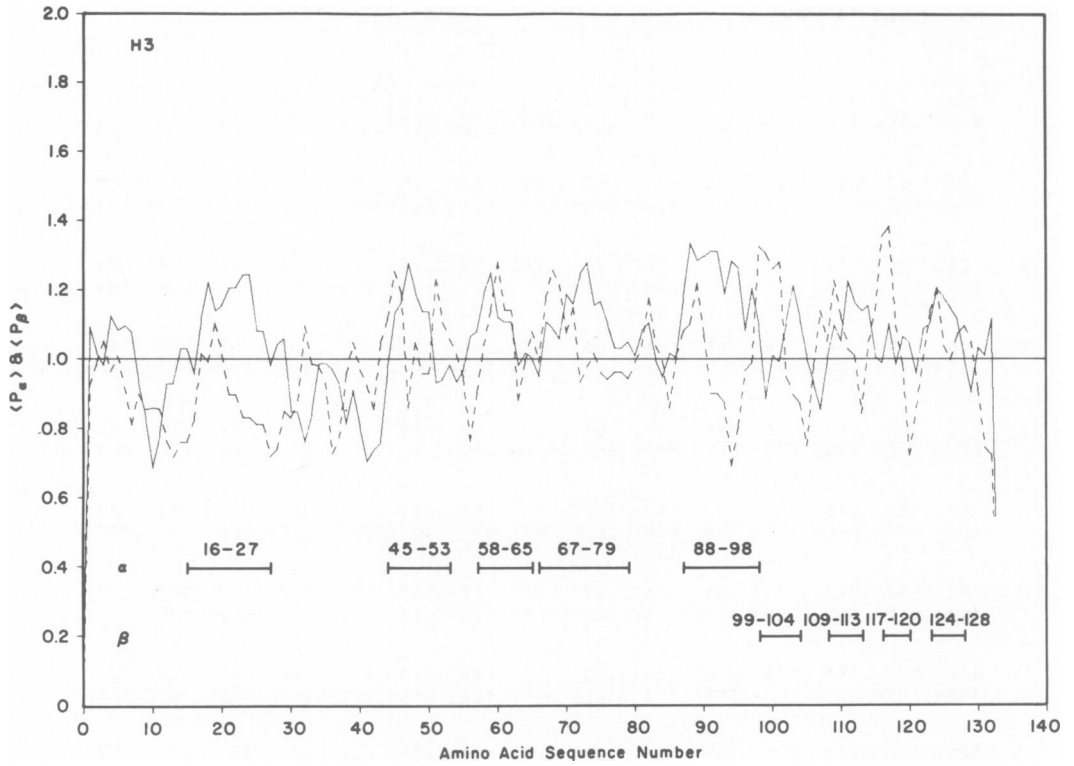

FIGURE 15 The conformational potential of H3. (——), helical potential $<P_\alpha>$ of tetrapeptide i to i + 3, (- - - -), β-sheet potential $<P_\beta>$ of tetrapeptide i to i + 3. Regions with helical and β-sheet-forming potential lie above the cut-off point 1.0 with tetrapeptide breakers falling below 1.0. The predicted α- and β-regions are underlined.

An indepth CD study on the oxidized (S-S) and reduced forms (SH) of H3 indicated differences in conformation (Adler, Moran, and Fasman, 1975). The reduced form was shown to have 4% α and 39% β in H_2O, while the oxidized form had 11% α and 29% β in H_2O. In 0.14 M NaF the reduced H3 had a 9% α, 39% β structure and the oxidized form had 15% α and 31% β (Table IV). D'Anna and Isenberg (1974*a*) showed for reduced H3 that salts cause a fast conformational change (14% α), followed by a slow change resulting in a final structure of 8% α and 24% β structure. At low temperatures the slow step could be inhibited.

The NMR data (Bradbury, Cary, et al., 1973) suggests that 50% of the molecule (68 residues) is in an ordered region between residues (42–110) (Table V). Within this sequence the prediction has four α-helices (41 residues), two β-sheets (11 residues), and four β-turns (13 residues), a total of 65 residues. Thus there is 96% agreement between the NMR data and the predicted structure in this region. Beyond this section there are one α-helix, two β-sheets, and four β-turns.

The predicted stable minimal helical content in H3 (unaffected by electrostatic repulsion) amounts to 16% α, agreeing well with the 15% α determined from CD for H3

TABLE IX

CONFORMATIONAL PREDICTION OF H3 COMPUTED FOR HELIX, β-SHEET, AND β-TURN REGIONS: $<P_\alpha>$, $<P_\beta>$, AND $<P_t>$ VALUES

H3	Calf thymus (prediction) 135 residues		
	Region*	$<P_\alpha>$†	$<P_\beta>$†
Helix	16–27 (12)	1.12	0.89
	45–53 (9)	1.12	1.09
	58–65 (8)	1.15	1.09
	67–79 (13)	1.15	1.07
	88–98 (11)	1.29	0.95
β-sheet	99–104 (6)	0.98	1.32
	109–113 (5)	1.08	1.16
	117–120 (4)	1.11	1.39
	124–128 (5)	1.16	1.15§

β-turn‖	Tetrapeptide	$<P_t>$†	$<P_\alpha>$†	$<P_\beta>$†
10–13	Ser-Thr-Gly-Gly	1.38	0.69	0.86
31–34	Ala-Thr-Gly-Gly	1.18	0.85	0.88
37–40	Lys-Pro-His-Arg	1.10	0.93	0.77
42–45	Arg-Pro-Gly-Thr	1.24	0.74	0.86
55–58**	Gln-Lys-Ser-Thr	1.09	0.97	0.95
84–87**	Phe-Gln-Ser-Ser	1.11	0.95	0.99
106–109	Asp-Thr-Asn-Leu	1.14	0.93	0.98
121–124	Pro-Lys-Asp-Ile	1.11	0.96	0.86

Helix: 39% β-turns: 24%
β-sheet: 15% Coil: 22%

*† See footnotes in Table I.

§This region is predicted as β despite the slightly higher helical potential since the β-turn prediction at 121–124 allows anti-parallel β-sheet formation with 117–120.

‖ Based on probability profile of Fig. 16.

**Predicted as β-turn since $<P_t> > <P_\alpha>$ and $<P_\beta>$.

(S—S) in 0.14 M NaF (Adler, Moran, and Fasman, 1975) and 14% α for H3 in phosphate buffer (D'Anna and Isenberg, 1974*a*). The predicted maximal β content in H3, due to $\alpha \rightarrow \beta$ transitions (Table VII), is 25% with 12% α (Table III). This predicted structure may correspond to the slow step aggregation of H3 (SH form) observed by D'Anna and Isenberg (1974*a*) which has a conformation of 8% α and 24% β. The NMR studies of Bradbury, Cary, et al. (1973) suggested that the region (42–110) was involved in interchain interactions while residues (1–41) are bound to DNA. All the stable helices (45–50), (58–65), and (88–95) are included in this structured region as well as β-sheets (99–104) and (109–113) (Fig. 17). Furthermore, the disruption of helix (16–27) by charge repulsion results in a "structureless" N-terminal region (1–44) containing 15 basic residues which may interact with the phosphates of DNA. In situ, the predicted β-turns at (10–13), (31–34), (37–40), and (42–45) in this "random" region (Fig. 17) may undergo specific folding upon complexation with DNA. The difference spectroscopy studies of H3 by Palau and Padros (1975) indicate that Tyr 99 is com-

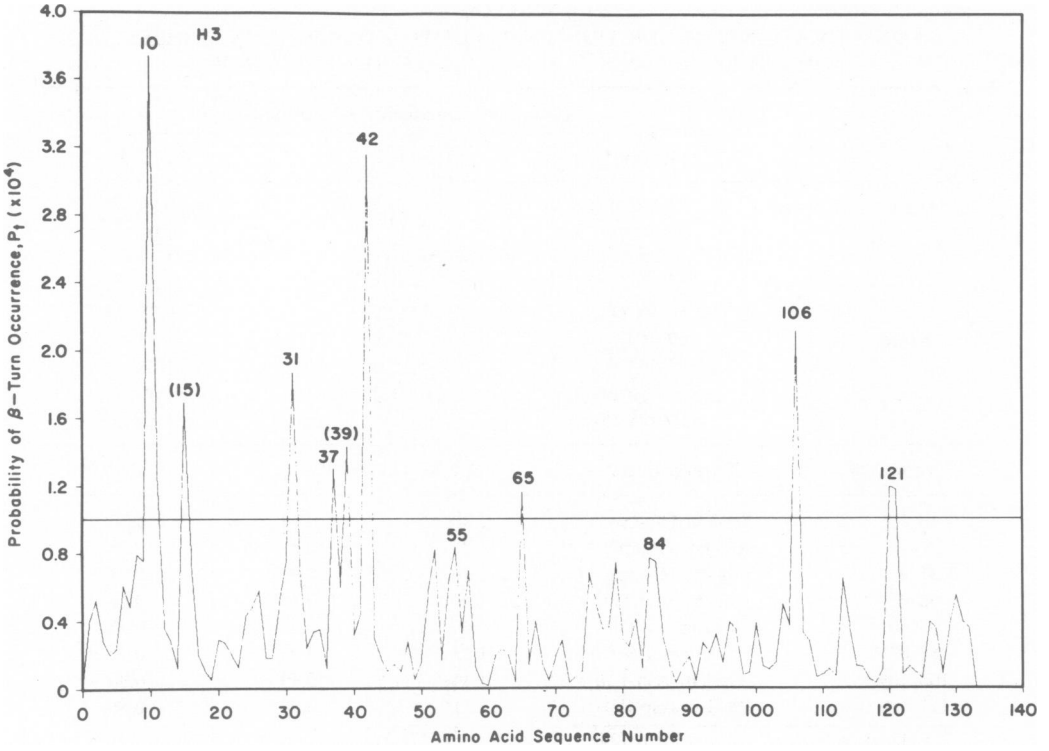

FIGURE 16 Probability of tetrapeptide β-turns in H3. The horizontal line corresponds to an arbitrary cut-off value of 1.0×10^{-4}. Of the nine sharp peaks above the cut-off, seven were predicted as β-turns, while two were excluded (residue number shown in parentheses) as belonging to other regions. In addition, two peaks below the cut-off were predicted as β-turns for reasons given in Table X.

pletely buried inside the histone molecule whereas Tyr 41 and Tyr 54 are more exposed and capable of interacting with the DNA backbone. An examination of the predicted model of H3 shows that Tyr 99 is indeed buried by neighboring helices and β-sheets while Tyr 41 and Tyr 54 are next to β-turns which are generally located on the surface of proteins.

H4: Prediction of the Secondary Structure

The complete sequence of H4 is shown in Fig. 18 (DeLange et al., 1968, 1969; Ogawa et al., 1969). The prediction conformational profile on α-helical and β-sheet sections is shown in Fig. 19. These sections are summarized in Table X and are composed of three α-helical regions of 28 residues, five β-sheet regions with 32 residues, and 45 residues in the random and β-turn conformation. The overall composition is: 28% α, 31% β, and 41% β-turn and/or random. There are nine specific β-turns deduced from the predictive profile, as seen in Fig. 20, and these are summarized in Table X, showing

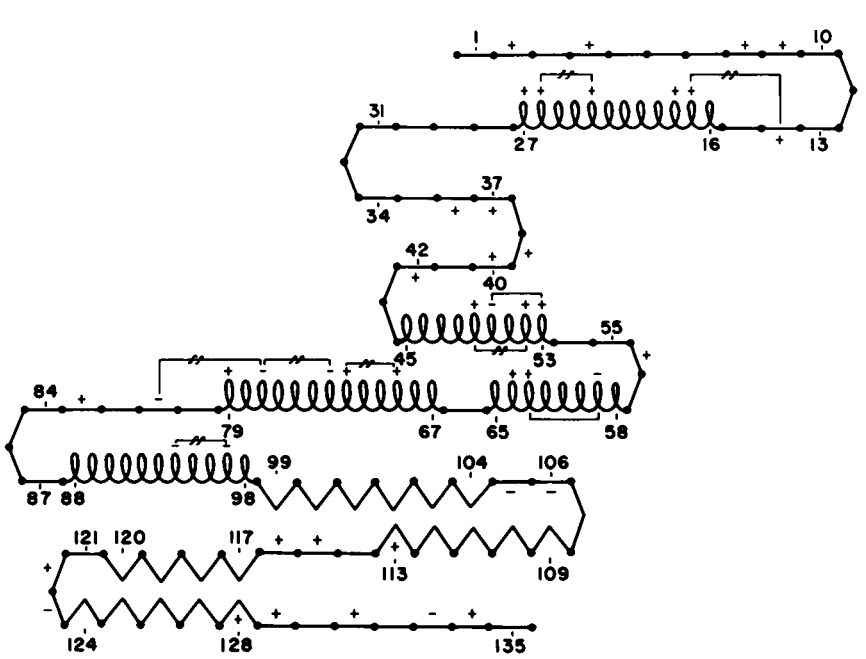

FIGURE 17 Schematic diagram of the secondary structure predicted for H3. Residues are represented as in the helical (ℓ), β-sheet ($\wedge$), and coil (——) conformation. Chain reversals indicate β-turn tetrapeptides. Helices with (⌐§§¬) contain charge repulsion between $i \pm 3$ or $i \pm 4$ residues and will be disrupted at low ionic strength, but are stabilized upon charge neutralization.

the 10 specific β-turns. These β-turns utilize 36% of the amino acid residues of the protein. Only 5% of the sequence is unstructured or random.

The schematic representation of the secondary structure is shown in Fig. 21. Four β-turns are predicted at the N-terminal region (1–14) due to their high probability of occurrence (see Fig. 20). This folding may be essential for bringing the positively charged residues 3, 5, 8, and 12 of H4 into a closer juxtaposition to the DNA-phosphates while the remaining portion of the molecule participates in histone-histone interaction. The β-turns (22–25) and (53–56) appear to stabilize α-β interactions while the β-turns (76–79) and (92–95) facilitate anti-parallel β-sheet formation within the H4 molecule (Fig. 21).

The charge distribution within the polypeptide chain is shown in Fig. 5. Two of the three helices predicted for the maximum secondary structure in H4 may be disrupted by charge repulsion. The remaining stable helix (57–67) and the five predicted β-sheets would yield the minimum secondary structure, of 11% α and 31% β (Table III).

The possible conformation changes are listed in Table VII. An $\alpha \rightarrow \beta$ transformation at residues (57–62) is a possibility since the β-potential is much higher than the α-potential ($<P_\beta> = 1.35 > <P_\alpha> = 1.14$) in this region. The newly formed

H4 - BOVINE 102 AMINO ACID RESIDUES

1	2	3	4	5	6	7	8	9	10	11	12	13	14	15
SER-	GLY-	ARG-	GLY-	LYS-	GLY-	GLY-	LYS-	GLY-	LEU-	GLY-	LYS-	GLY-	GLY-	ALA-
16	17	18	19	20	21	22	23	24	25	26	27	28	29	30
LYS-	ARG-	HIS-	ARG-	LYS-	VAL-	LEU-	ARG-	ASP-	ASN-	ILE-	GLN-	GLY-	ILE-	THR-
31	32	33	34	35	36	37	38	39	40	41	42	43	44	45
LYS-	PRO-	ALA-	ILE-	ARG-	ARG-	LEU-	ALA-	ARG-	ARG-	GLY-	GLY-	VAL-	LYS-	ARG-
46	47	48	49	50	51	52	53	54	55	56	57	58	59	60
ILE-	SER-	GLY-	LEU-	ILE-	TYR-	GLU-	GLU-	THR-	ARG-	GLY-	VAL-	LEU-	LYS-	VAL-
61	62	63	64	65	66	67	68	69	70	71	72	73	74	75
PHE-	LEU-	GLU-	ASN-	VAL-	ILE-	ARG-	ASP-	ALA-	VAL-	THR-	TYR-	THR-	GLU-	HIS-
76	77	78	79	80	81	82	83	84	85	86	87	88	89	90
ALA-	LYS-	ARG-	LYS-	THR-	VAL-	THR-	ALA-	MET-	ASP-	VAL-	VAL-	TYR-	ALA-	LEU-
91	92	93	94	95	96	97	98	99	100	101	102			
LYS-	ARG-	GLN-	GLY-	ARG-	THR-	LEU-	TYR-	GLY-	PHE-	GLY-	GLY-			

FIGURE 18 The amino acid sequence of histone H4 (bovine), as determined by DeLange et al. (1969).

β-(57–62) can then easily interact with β-(46–51) to form an anti-parallel β-sheet with the aid of β-turn (53–56).

H4: Physical-Chemical Studies; Correlation with Predicted Structure; ORD, CD, NMR

The ORD studies during the 1960s indicated that H4 had a random structure in aqueous media (Bradbury et al., 1965; Oh, 1970) and the helicity increased at higher ionic strength (1.0 M NaCl, 22% α) (Bradbury et al., 1965).

The conformation at low ionic strength, determined by CD studies, was 7% α, 38% β (Fasman et al., 1970) and at higher ionic strength was 19% α and 30% β (Shih and Fasman, 1971; Adler et al., 1975*b*) (Table IV). These results vary with the standards used to evaluate the CD curves. In 95% MeOH the molecule has 8% α and 33% β (Adler, Fulmer, and Fasman, 1975). In the presence of phosphate two steps in the folding of H4 were detected (D'Anna and Isenberg, 1973; Wickett et al., 1972; Smerdon and Isenberg, 1973, 1974; Li et al., 1972). The fast step produced a 15% α-conformation which was followed by a slow step yielding 15% α and 32% β, in good agreement with the above. The slow step could be inhibited at a low temperature, and may be involved in intermolecular association of dimers. The salt-induced changes have been confirmed (Pekary et al., 1975*a*, *b*) and by utilizing both infrared and CD an estimate of 25% α-helical structure of H4 (in 200 mM NaCl) was made (Lewis et al., 1975). NMR studies on H4 indicate a structured region from (33–102) (Boublik et al.,

TABLE X

CONFORMATIONAL PREDICTION OF H4 COMPUTED FOR HELIX, β-SHEET, AND β-TURN REGIONS: $<P_\alpha>$, $<P_\beta>$, AND $<P_t>$ VALUES

H4	Bovine (prediction) 102 residues		
	Region*	$<P_\alpha>$†	$<P_\beta>$†
Helix	15–22 (8)	1.12	1.00
	31–39 (9)	1.09	0.96
	57–67 (11)	1.10	1.24§
β-sheet	26–30 (5)	0.93	1.25
	46–51 (6)	0.90	1.25
	69–73 (5)	0.97	1.28
	80–90 (11)	1.09	1.23
	96–100 (5)	0.89	1.22

β-turn ‖	Tetrapeptide	$<P_t>$†	$<P_\alpha>$†	$<P_\beta>$†
2–5	Gly-Arg-Gly-Lys	1.26	0.82	0.79
4–7	Gly-Lys-Gly-Gly	1.42	0.72	0.75
7–10	Gly-Lys-Gly-Leu	1.18	0.88	0.89
11–14	Gly-Lys-Gly-Gly	1.42	0.72	0.75
22–25	Leu-Arg-Asp-Asn	1.14	0.97	0.91
39–42	Arg-Arg-Gly-Gly	1.25	0.77	0.84
53–56**	Glu-Thr-Arg-Gly	1.05	0.97	0.81
76–79††	Ala-Lys-Arg-Lys	0.90	1.18	0.81
92–95	Arg-Gln-Gly-Arg	1.10	0.91	0.93

Helix: 28% β-turns: 36%
β-sheet: 31% Coil: 5%

*† See footnotes in Table I.

§ This region is predicted as helical despite its higher β-potential since hierarchical conformational analysis shows $(H_3h_6Ib)_\alpha$ and $(H_4h_3i_2bB)_\beta$.

‖ Based on probability profile of Fig. 20.

** Predicted as β-turn since $<P_t> > <P_\alpha>$ and $<P_\beta>$.

†† The β-turn probability at 76–79 (Fig. 20) is slightly above average ($<p_t> = 5.0 \times 10^{-5}$) though below the cut-off point of 1.0×10^{-4}. Nevertheless a β-turn is predicted at this position to allow possible anti-parallel β-sheet interactions between regions 69–73 and 80–90.

1970; Bradbury and Rattle, 1972) (Table V); however, this has been challenged, and an estimate of structure only in the ~(70–80)–102 region has also been postulated (Pekary et al., 1975*a*, *b*). These studies confirm the aggregation of H4 at higher ionic strength.

The conformation of H4 in association with DNA has been investigated (Shih and Fasman, 1971, 1972; Wagner, 1970; Wagner and Vandergift, 1972; Li et al., 1971). In association with DNA or polyvinylphosphate the conformation of H4 became more helical. Removal of 18 amino acids from the C-terminus prevented aggregation and binding to DNA (Ziccardi and Schumaker, 1973). This cleaved fragment (85–102) is part of the anti-parallel β-sheet predicted at the C-terminal (Fig. 21) and is a likely site for aggregation. The acetylated H4 species, mono, di, or higher, is less effective in producing conformational distortions of DNA; this finding may be relevant to mecha-

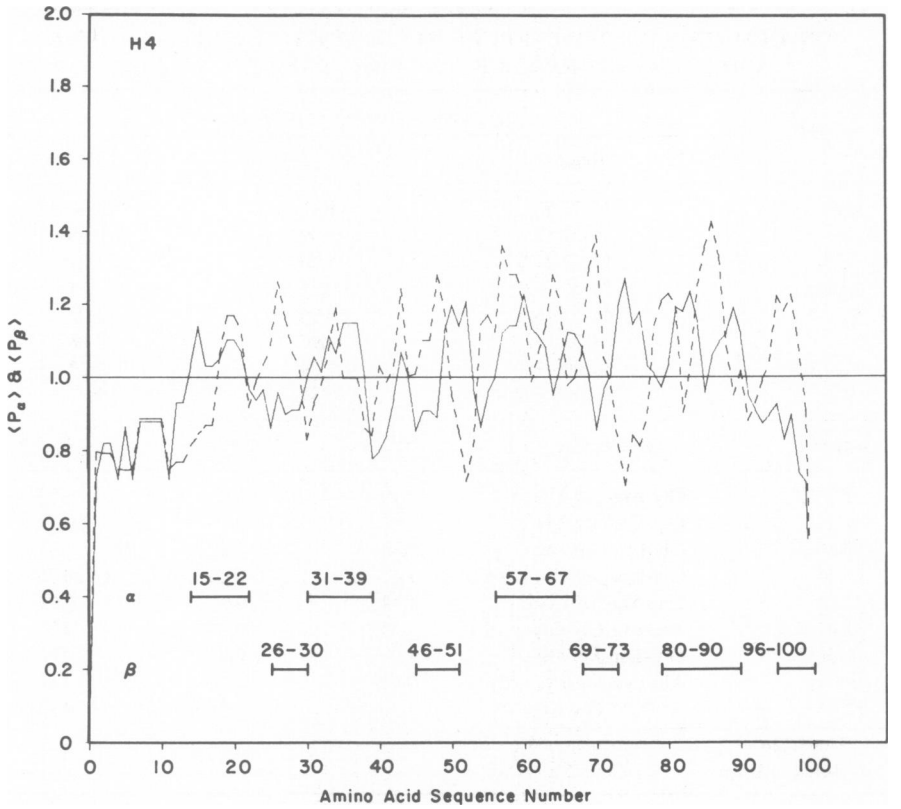

FIGURE 19 The conformational potential of H4. (——), helical potential $<P_\alpha>$ of tetrapeptide i to i + 3. (- - - -), β-sheet potential $<P_\beta>$ of tetrapeptide i to i + 3. Regions with helical and β-sheet-forming potential lie above the cut-off point 1.0 with tetrapeptide breakers falling below 1.0. The predicted α- and β-regions are underlined.

nisms of genetic regulation (Adler, Ross, et al., 1974). Electron microscopy of H4:DNA complexes showed large globular aggregates (Slayter et al., 1972).

The NMR data (Bradbury and Rattle, 1972) suggests an ordered region between (33–102), that is 69% of the sequence is structured. Within this region 62 of the 70 residues (89%) are predicted as being in definitive structures (two α-helices, 20 residues; four β-sheets, 27 residues, and five β-turns, 15 residues). The CD estimate of conformation yields 19% α and 30% β in 0.14 M NaCl (Adler, Fulmer, and Fasman, 1975), while in phosphate buffer an estimate of 15% α and 32% β was made (Wickett et al., 1972). Thus the predicted value for the β-sheet is remarkably close, while the α-helix prediction is higher than that found under the conditions used. However, of the two unstable helices (Fig. 21) predicted, one lies outside and the other is at the boundary of the NMR structured region (33–102). Since the predicted stable helix (57–67) lies within the structured region, the predicted conformation of H4 agrees well with the NMR data.

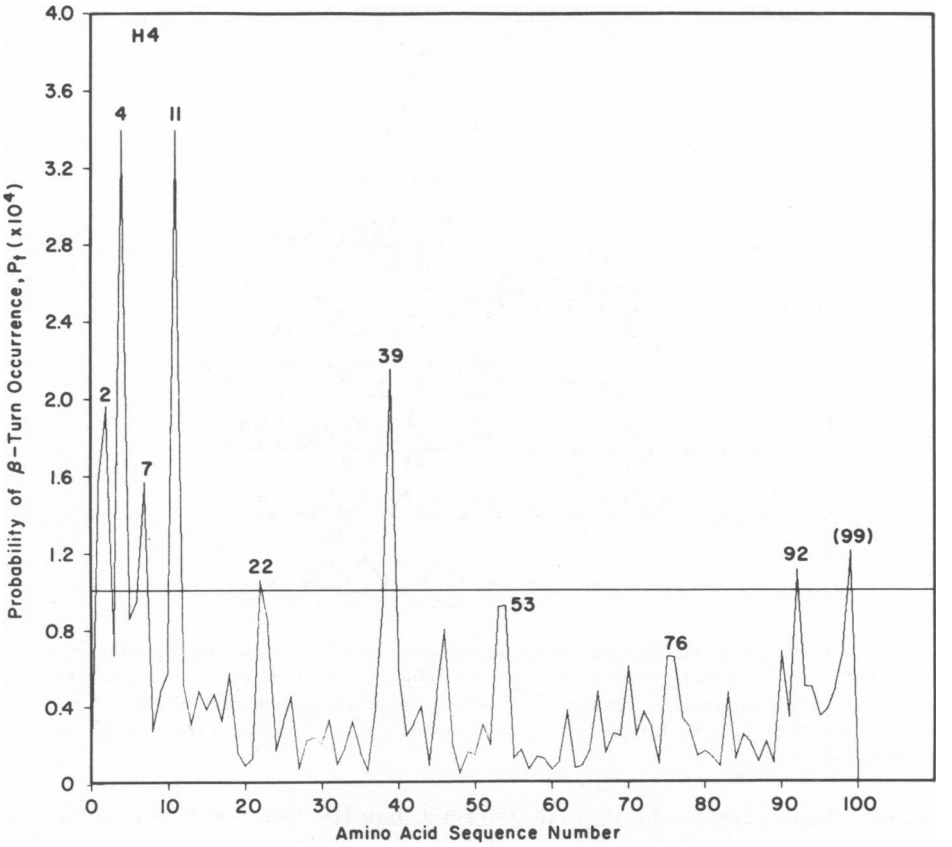

FIGURE 20 Probability of tetrapeptide β-turns in H4. The horizontal line corresponds to an arbitrary cut-off value of 1.0×10^{-4}. Seven of the eight sharp peaks above the cut-off were predicted as β-turns while residue 99 was excluded as belonging to a β-sheet region. Two peaks below the cut-off were predicted as β-turns for reasons given in Table 10.

The minimal secondary predicted structure of H4 (11% α, 31% β) is in good agreement with the CD findings (Table IV). The observation (Diggle and Peacocke, 1971; Edwards and Shooter, 1969) that H4 is the most strongly aggregating of the histones may be explained by the greater amounts of β-sheets predicted in H4 than in the other histones. From NMR, CD, and IR studies of H4 and its fragments, Lewis et al. (1975) concluded that the region (25–67) is essential for the folding and self-association of H4 while the C-terminal residues (74–102) are involved in β-sheet aggregation. The 21% β (9 residues) and 28% α (12 residues) found experimentally for the fragment (25–67) (Lewis et al., 1975) correlate well with the predicted conformation (Fig. 21) in this region: β sheets (26–30) and (46–51) (11 β-residues) and stable helix (57–67) (11 α-residues). From NMR studies of H4 and its fragment (85–102) Pekary et al., (1975*a*) found that the last 20–30 residues of the C-terminus are involved in rigid secondary structure, thus confirming the predicted anti-parallel β-sheets at the C-terminus of H4.

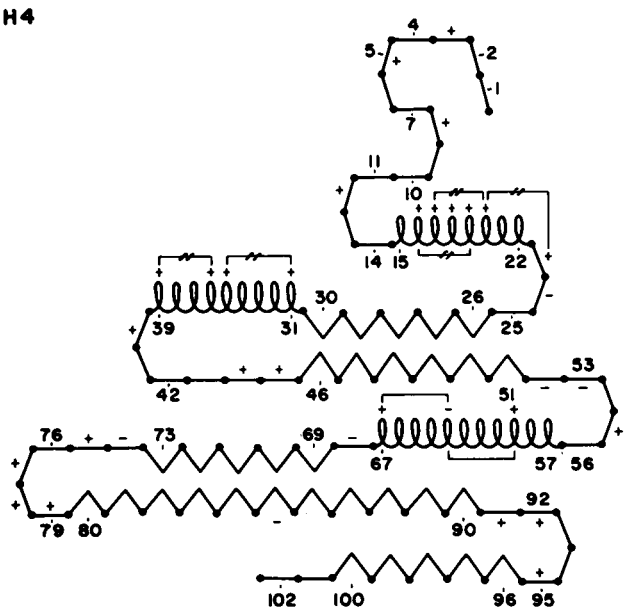

FIGURE 21 Schematic diagram of the secondary structure predicted for H4. Residues are represented as in the helical (ℓ), β-sheet ($\wedge$), and coil (——) conformation. Chain reversals indicate β-turn tetrapeptides. Helices with (⌐ƒƒ¬) contain charge repulsion between $i \pm 3$ or $i \pm 4$ residues and will be disrupted at low ionic strength, but are stabilized upon charge neutralization.

However, their interpretation that His 75 rather than His 18 is involved in conformational change with increasing ionic strength may be questioned. From the predicted model (Fig. 21), His 75 is in a random conformation and next to β-turn (76–89) while His 18 is located in helix (15–22) which contains many electrostatic repulsions. Hence, it is more likely that His 18 participates in the conformational transitions of helix (15–22) which is dependent on ionic strength.

Histone:Histone Interactions

The discovery of associated histones in complexes along the DNA chain in situ (Olins and Olins, 1974; Kornberg, 1974; Lohr and Van Holde, 1975), the isolation of such complexes (Roark et al., 1974; Skandrani et al., 1967; Kelley, 1973), the ability to cross link histones in situ (Kornberg, 1974; Van Lente et al., 1975; Hyde and Walker, 1975), and the ability to reconstitute such complexes (see reviews, Van Holde and Isenberg, 1975; Rubin and Mourdrianakis, 1975; Sperling and Bustin, 1975) has firmly established the importance of such interactions in chromatin.

Isenberg and associates have performed elegant studies of the cross reactions of histone-histone association (see review, Van Holde and Isenberg, 1975). They have also evaluated the conformational consequences of such interactions. The change in secondary structures upon association can be summarized as follows: upon interaction of H4 and H3 an increase in 1.9% α is found; H2B and H2A interaction produces a

5.9% increase in α-helix, and H2B and H4 interaction causes a 3.5% α increase. No change in β structure could be observed in any of these interactions.

The H3–H4 complex is the most stable complex (D'Anna and Isenberg, 1974*c*). Examination of the schematic diagrams for H3 and H4 (Fig. 17 and 21) reveals that both these histones have a large β-sheet content in the COOH-terminus. H3 has β-sheets in regions (99–104), (109–113), (117–120), and (124–128). The NMR data suggests an ordered structure between (42–110) in the H3 monomer. H4 has β-sheets in regions (69–73), (80–90), and (96–100). The NMR data suggests an ordered region in section (33–102). It is proposed that intermolecular β-sheets interactions are involved in the COOH-termini associations of H3 and H4. β-sheet:β-sheet interactions between monomer units have frequently been observed in associating protein systems. Such interactions are found between the monomer units in crystalline insulin (Blundell et al., 1972) and in concanavalin A (Hardman and Ainsworth, 1972). The conformational changes suggested for H3 (Table VII) also allow two helical sections (45–53) and (67–79) to transform to three β-sheets (45–48), (67–71), and (74–78). If these changes were to occur upon association with another histone, more β-sheet would be available for intermolecular β-sheet formation. β:β interactions offer greater stability than α-helix:α-helix interaction since the former allows for hydrogen bonding as well as side-chain:side-chain (hydrophobic) stabilization, while α-helix:α-helix association allows only the latter interaction. For this reason intermolecular β-sheet interactions are preferred as they offer greater stability. Possible conformational changes in H4 (Table VII) allows one helix (57–67) to transform to a β-sheet (57–62), thus enhancing the potential for β:β association with H3.

Another histone pair which associate in a 1:1 stochiometry is H2A:H2B (D'Anna and Isenberg, 1974*c*). Both of these histones have their α- and β-sections evenly distributed through their polypeptide chains (Figs. 9 and 13 and Tables VI and VIII). However, there are β-sections in the center regions [H2A (23–27), (30–34); H2B (39–48), (61–66)] which may associate, as well as β regions in the COOH-terminus of each [H2A (76–79), (100–104), and (111–116); H2B (88–90) and (117–122)] which might likewise interact.

Conformational $\alpha \rightarrow \beta$ transitions allow three new β-regions [(49–55), (57–63), and (83–87)] to form in H2A and one new β-section (94–102) in H2B (Table VII). These new β-regions offer additional sites for β:β interaction.

H2B:H4 have an association constant of $K = 10^6\ M^{-1}$ (D'Anna and Isenberg, 1973). Both these polypeptide chains have random structures at the NH_2-termini (Figs. 13 and 21), with β-sheets at both the center regions and COOH-termini. Hence β:β interactions may be involved in these regions during the association of H2B and H4. Furthermore, the $\alpha \rightarrow \beta$ transition at (57–62) in H4 provides an additional site for association with H2B.

Examination of the conformation of several proteins whose structure has been determined by X-ray crystallography reveals some interesting structural phenomena shared by all these proteins. β-sheet interactions frequently are responsible for the core structure, comprising the center, which is hydrophobic in nature, while the α-helices are

packed around these cores making up the outer, hydrophilic topology. It was found (Chou and Fasman, 1974*a*, *b*) that β-sheets rarely have charged amino acids in their chains, while α-helices often have one side hydrophobic and the other side composed of charged residues. Thus, the α-helices hydrophobic surface often interacts with the β-sheet core, while their charged surface makes up the outer surface and interacts with the aqueous medium. Such packing should be kept in mind when speculative proposals are made concerning histone:histone interactions.

CONCLUSIONS

The prediction of the conformation of the individual histones permits a detailed description of likely α-helices, β-sheets, and β-turns in these proteins. This method can specify which structures are most probably under various environmental conditions, from changes in ionic strength to association between histones and in association with DNA. The predictions allow a more detailed description of regions of structure than possible by NMR and CD analysis. Potential conformational changes are predicted and sites for histone:histone association may be speculated upon.

Great progress has been made in our understanding of the chromatin complex, and great promise is offered by the neutron scattering technique now being undertaken (e.g., Baldwin et al., 1975), as well as X-ray crystallography. However, until these techniques solve the problem of chromatin organization, understanding of the architecture of chromatin, and of its biological mechanisms and regulation, will rely strongly on the understanding of the conformation of its components. Thus the predictions herein offer one approach to the final unraveling of the structure of chromatin.

We are grateful to Professor R. D. Cole for the sequence of RTL-3H and Professor G. Dixon for the sequence of trout testis H1 prior to publication.

The authors gratefully acknowledge the support, in part, by grants from the U. S. Public Health (GM 17533), National Science Foundation (GB 29204X), and the American Cancer Society (P577).

This is publication no. 1086 of the Graduate Department of Biochemistry, Brandeis University, Waltham, Mass. 02154.

Received for publication 24 March 1976.

REFERENCES

ADLER, A. J., and G. D. FASMAN. 1971. Circular dichroism studies of lysine-rich histone f-1:deoxyribonucleic acid complexes. Effects of salts and dioxane upon conformation. *J. Phys. Chem.* **75**:1516.

ADLER, A. J., G. D. FASMAN, L. J. WANGH, and V. G. ALLFREY. 1974. Altered conformational effects of naturally acetylated histone f2al (IV) in f2al:deoxyribonucleic acid complexes. Circular dichroism studies. *J. Biol. Chem.* **249**:2911.

ADLER, A. J., A. W. FULMER, and G. D. FASMAN. 1975. Interaction of histone f2al fragments with deoxyribonucleic acid. Circular dichroism and thermal denaturation studies. *Biochemistry.* **14**:1445.

ADLER, A. J., T. A. LANGAN, and G. D. FASMAN. 1972. Complexes of deoxyribonucleic acid with lysine-rich (f1) histone phosphorylated at two separate sites: circular dichroism studies. *Arch. Biochem. Biophys.* **153**:769.

ADLER, A. J., E. C. MORAN, and G. D. FASMAN. 1975. Complexes of DNA with histone f2a2 and f3. Circular dichroism studies. *Biochemistry.* **14**:4179.

ADLER, A. J., D. G. ROSS, K. CHEN, P. A. STAFFORD, M. J. Woiszwillo, and G. D. FASMAN. 1974. Interaction of deoxyribonucleic acid with histone f2b and its half-molecules: circular dichroism studies. *Biochemistry.* **13**:616.

ADLER, A. J., B. SCHAFFHAUSEN, T. A. LANGAN, and G. D. FASMAN. 1971. Altered conformational effects of phosphorylated lysine-rich histone (f-1) in f-1:deoxyribonucleic acid complexes. Circular dichroism and immunological studies. *Biochemistry.* **10**:909.

ANDERSON, R. A., Y. NAKASHIMA, and J. E. COLEMAN. 1975. Chemical modifications of functional residues of fd gene 5 DNA-binding protein. *Biochemistry.* **14**:907.

BALDWIN, J. P., P. G. BOSELEY, E. M. BRADBURY, and K. IBEL. 1975. The subunit structure of the eukaryotic chromosome. *Nature (Lond.).* **253**:245.

BLUNDELL, T., G. DODSON, D. HODGKIN, and D. MERCOLA. 1972. Insulin: the structure in the crystal and its reflection in chemistry and biology. *Adv. Protein Chem.* **26**:279.

BOUBLIK, M., E. M. BRADBURY, and C. CRANE-ROBINSON. 1970. An investigation of the conformational changes of histones Fl and F2al by proton magnetic resonance spectroscopy. *Eur. J. Biochem.* **14**:486.

BOUBLIK, M., E. M. BRADBURY, C. CRANE-ROBINSON, and E. W. JOHNS. 1970. An investigation of the conformational changes of histone F2b by high resolution nuclear magnetic resonance. *Eur. J. Biochem.* **17**:151.

BOUBLIK, M., E. M. BRADBURY, C. CRANE-ROBINSON, and H. W. E. RATTLE. 1971. Proton magnetic resonance studies of the interactions of histone Fl and F2B with DNA. *Nature (Lond.).* **229**:149.

BRADBURY, E. M., B. G. CARPENTER, and H. W. E. RATTLE. 1973. Magnetic resonance studies of deoxyribonucleoprotein. *Nature (Lond.).* **241**:123.

BRADBURY, E. M., P. D. CARY, G. E. CHAPMAN, C. CRANE-ROBINSON, S. E. DANBY, and H. E. W. RATTLE. 1975. Studies on the role and mode of operation of the very-lysine-rich histone Hl (Fl). The conformation of histone Hl. *Eur. J. Biochem.* **52**:605.

BRADBURY, E. M., P. D. CARY, C. CRANE-ROBINSON, and H. W. E. RATTLE. 1973. Conformations and interactions of histones and their role in chromosome structure. *Ann. N.Y. Acad. Sci.* **222**:266.

BRADBURY, E. M., P. D. CARY, C. CRANE-ROBINSON, H. W. E. RATTLE, M. BOUBLIK, and P. SAUTIERE. 1975. Conformations and interactions of histone H2A (F2a2, ALK). *Biochemistry.* **14**:1876.

BRADBURY, E. M., P. D. CARY, C. CRANE-ROBINSON, P. L. RICHES, and E. W. JOHNS. 1972. Nuclear-magnetic resonance and optical-spectroscoptic studies of conformation and interactions in the cleaved halves of histone F2B. *Eur. J. Biochem.* **26**:482.

BRADBURY, E. M., G. E. CHAPMAN, S. E. DANBY, P. G. HARTMAN, and P. L. RICHES. 1975. Studies on the role and mode of operation of the very-lysine-rich histone Hl (Fl) in eukaryote chromatin. The properties of the N-terminal and C-terminal halves of histone Hl. *Eur. J. Biochem.* **57**:521.

BRADBURY, E. M., C. CRANE-ROBINSON, H. GOLDMAN, H. W. E. RATTLE, and R. M. STEPHENS. 1967. Spectroscopic studies of the conformation of histones and protamine. *J. Mol. Biol.* **29**:507.

BRADBURY, E. M., C. CRANE-ROBINSON, D. M. P. Phillips, E. W. JOHNS, and K. MURRAY. 1965. Conformational investigations of histones. *Nature (Lond.).* **205**:1315.

BRADBURY, E. M. and H. W. E. RATTLE. 1972. Simple computer-aided approach for the analysis of the nuclear-magnetic resonance spectra of histones. Fractions Fl, F2al, cleavage halves of F2B and F2B-DNA. *Eur. J. Biochem.* **27**:270.

BURNOTTE, J., B. D. STOLLAR, and G. D. FASMAN. 1973. Immunological and circular dichroism studies of maleylated f-1 (A) histone and complexes with DNA. *Arch. Biochem. Biophys.* **155**:428.

BUSTIN, M., S. C. RALL, R. H. STELLWAGEN, and R. D. COLE. 1969. Histone structure: asymmetric distribution of lysine residues in lysine-rich histone. *Science (Wash. D.C.).* **163**:391.

CHEN, Y-H., J. T. YANG, and H. M. MARTINEZ. 1972. Determination of the secondary structures of proteins circular dichroism and optical rotatory dispersion. *Biochemistry.* **11**:4120.

CHOU, P. Y., A. J. ADLER, and G. D. FASMAN. 1975. Conformational prediction and circular dichroism studies on the *lac* repressor. *J. Mol. Biol.* **96**:29.

CHOU, P. Y., and G. D. FASMAN. 1974*a*. Conformational parameters for amino acids in helical, β-sheet and random coil regions calculated from proteins. *Biochemistry.* **13**:211.

CHOU, P. Y., and G. D. FASMAN. 1974*b*. Prediction of protein conformation. *Biochemistry.* **13**:222.

CHOU, P. Y., and G. D. FASMAN. 1975. The conformation of glucagon: predictions and consequences. *Biochemistry.* **14**:2536.

CLARK, V. M., D. M. J. LILLEY, O. W. HOWARD, B. M. RICHARDS, and J. F. PARDON. 1974. The Structure and properties of histone F2a comprising the heterologous group F2a1 and F2a2 studies by ^{13}C nuclear magnetic resonance. *Nucleic Acids Res.* **1**:865.

D'ANNA, JR., J. A., and I. ISENBERG. 1972. Fluorescence anisotropy and circular dichroism study of conformational changes in histone IIb2. *Biochemistry.* **11**:4017.

D'ANNA, JR., J. A., and I. ISENBERG. 1973. A complex of histones IIb2 and IV. *Biochemistry.* **12**:1035.

D'ANNA, JR., J. A., and I. ISENBERG. 1974*a*. Conformational changes of histone ARE (F3, III). *Biochemistry.* **13**:4987.

D'ANNA, JR., J. A., and I. ISENBERG. 1974*b*. Conformational changes of histone LAK (f2a2). *Biochemistry.* **13**:2093.

D'ANNA, JR., J. A., and I. ISENBERG. 1947*c*. A histone cross-complexing pattern. *Biochemistry.* **13**:4992.

DELANGE, R. J., D. M. FAMBROUGH, E. L. SMITH, and J. BONNER. 1969. Calf and pea histone IV. *J. Biol. Chem.* **224**:319.

DELANGE, R. J., J. A. HOOPER, and E. L. SMITH. 1972. Complete amino-acid sequence of calf-thymus histone III. *Proc. Natl. Acad. Sci. U.S.A.* **69**:882.

DELANGE, R. J., E. L. SMITH, D. M. FAMBROUGH, and J. BONNER. 1968. Amino acid sequence of histone IV: presence of ϵ-N-acetyl-lysine. *Proc. Natl. Acad. Sci. U.S.A.* **61**:1145.

DIGGLE, J. H., and A. R. PEACOCKE. 1971. The molecular weights and association of the histones of chicken erythrocytes. *FEBS Lett.* **18**:138.

DUNN, B. M., and I. M. CHAIKEN. 1975. Relationship between α-helical propensity and formation of the ribonuclease-S complex. *J. Mol. Biol.* **95**:497.

EDWARDS, P. A., and K. V. SHOOTER. 1969. Ultracentrifuge studies of histone fractions from calf thymus deoxyribonucleoprotein. *Biochem. J.* **114**:227.

ELGIN, S. C. R., S. FROEHNER, J. E. SMART, and J. Bonner. 1971. The biology and chemistry of chromosomal proteins. *Adv. Cell Mol. Biol.* **1**:1.

ELGIN, S. C. R., and H. WEINTRAUB. 1975. Chromosomal proteins and chromatin structure. *Ann. Rev. Biochem.* **44**:726.

FASMAN, G. D., P. Y. CHOU, and A. J. ADLER. 1976. Histone conformation: predictions and experimental studies. *In* Molecular Biology of the Mammalian Apparatus—Its Relationship to Cancer, Aging and Medical Genetics. P.O.P. Ts'o, editor. Associated Scientific Publishers, Elsevier Excerpta Medica North-Holland, Amsterdam. In press.

FASMAN, G. D., B. SCHAFFHAUSEN, L. GOLDSMITH, and A. ADLER. 1970. Conformational changes associated with F-1 histone: deoxyribonucleic acid complexes. Circular dichroism studies. *Biochemistry.* **9**:2814.

FASMAN, G. D., M. S. VALENZUELA, and A. J. ADLER. 1971. Complexes of deoxyribonucleic acid with fragments of lysine-rich histone (f-1). Circular dichroism studies. *Biochemistry.* **10**:3795.

FITZSIMONS, D. W., and G. E. W. WOLSTENHOLME, editors. 1975. The structure and function of chromatin. *Ciba Found. Symp.* 28.

GAREL, A., A. M. KOVACS, M. CHAMPAGNE, and M. DAUNE. 1975*a*. Comparison between histones Fv and F2a2 of chicken erythrocyte. I. Structure, stability and conformation of the free proteins. *Biochim. Biophys. Acta.* **395**:5.

GAREL, A., A. M. KOVACS, M. CHAMPAGNE, and M.DAUNE. 1975*b*. Comparison between histones FV and F2a2 of chicken erythrocytes. II. Interaction with homologous DNA. *Biochim. Biophys. Acta.* **395**:16.

GREENFIELD, N.J., and G.D. FASMAN. 1969. Computed circular dichroism spectra for the evaluation of protein conformation. *Biochemistry.* **8**:4108.

HARDMAN, K. D., and C. F. AINSWORTH. 1972. Structure of concanavalin Å at 2.4 A resolution. *Biochemistry.* **11**:4910.

HYDE, J. E., and I. O. WALKER. 1975. Covalent cross-linking of histones in chromatin. *FEBS Lett.* **50**:150.

IWAI, K., K. ISHIKAWA, and H. HAYASHI. 1970. Amino acid sequence of slightly lysine-rich histone. *Nature (Lond.).* **226**:1056.

JIRGENSONS, B., and L. S. HRILICA. 1965. The conformational changes of calf thymus histone fractions as determined by optical rotatory dispersion. *Biochim. Biophys. acta.* **109**:241.

JONES, G. M. T., S. C. RALL, and R. D. COLE. 1974. Extension of the amino acid sequence of a lysine-rich histone. *J. Biol. Chem.* **249**:2548.

KELLEY, R. I. 1973. Isolation of a histone IIbl-IIb2 complex. *Biochem. Biophys. Res. Commun.* **54**: 1588.

KORNBERG, R. D. 1974. Chromatin structure: A repeating unit of histones and DNA. *Science* (*Wash, D.C.*). **184**:868.

KORNBERG, R. D., and J. O. THOMAS. 1974. Chromatin structure: oligomers of the histones. *Science* (*Wash. D.C.*). **184**:865.

LEWIS, P. N., and E. M. BRADBURY. 1974. Effect of electrostatic interactions on the prediction of helices in protein. The histones. *Biochim. Biophys. Acta.* **336**:153.

LEWIS, P. N., E. M. BRADBURY, and C. CRANE-ROBINSON. 1975. Ionic strength induced structure in histone H4 and its fragments. *Biochemistry.* **14**:3391.

LI, H. J., I. ISENBERG, and W. C. JOHNSON, JR. 1971. Absorption and circular dichroism studies on nucleohistone IV. *Biochemistry.* **10**:2587.

LI, H. J., R. WICKETT, A. M. CRAIG, and I. ISENBERG. 1972. Conformational changes in histone IV. *Biopolymers.* **11**:375.

LIM, V. I. 1974. Structural principles of the globular organization of protein chains. A stereochemical theory of globular protein secondary structure. *J. Mol. Biol.* **88**:857.

LOHR, D., and K. E. VAN HOLDE. 1975. Yeast chromatin subunit structure. *Science* (*Wash. D.C.*). **188**: 165.

MATTHEWS, B. W. 1975. Comparison of the predicted and observed secondary structure of T4 phage lysozyme. *Biochim. Biophys. Acta.* **405**:442.

MAXFIELD, F. R., and H. A. SCHERAGA. 1975. The effect of neighboring charges on the helix forming ability of charged amino acids in proteins. *Macromolecules.* **8**:491.

OGAWA, Y., G. QUAGLIAROTTI, J. JORDON, C. W. TAYLOR, W. C. STARBUCK, and H. BUSCH. 1969. Structural analysis of the glycine-rich, arginine-rich histone III. Sequence of the amino-terminal half of the molecule containing the modified lysine residues and the total sequence. *J. Biol. Chem.* **244**: 4387.

OH, Y. H. 1970. Spectroscopic studies of five purified histones from calf thymus. *J. Biol. Chem.* **245**:6404.

OLINS, A. L., and D. E. OLINS. 1974. Spheroid chromatin units (ν Bodies). *Science* (*Wash. D.C.*). **183**: 330.

PALAU, J., and E. PADROS. 1975. Behaviour of tyrosyl residues of calf thymus histone F-3. *Eur. J. Biochem.* **52**:555.

PALAU, J., and P. PUIGDOMENECH. 1974. The structural code for proteins: zonal distribution of amino acid residues and stabilization of helices by hydrophobic triplets. *J. Mol. Biol.* **88**:457.

PEKARY, A. E., S. I. CHAN, C. J. HSU, and T. WAGNER. 1975*a*. Nuclear magnetic resonance studies on the solution conformation of histone IV fragments obtained by cyanogen bromide cleavage. *Biochemistry.* **14**:1184.

PEKARY, A. E., H. J. LI, S. I. CHAN, C. J. HSU, and T. E. WAGNER. 1975*b*. Nuclear magnetic resonance studies of histone IV solution conformation. *Biochemistry.* **14**:1177.

RALL, S. C., and R. D. COLE. 1971. Amino acid sequence and sequence variability of the amino-terminal regions of the lysine-sequence variability of the amino-terminal regions of the lysine-rich histones. *J. Biol. Chem.* **246**:7175.

ROARK, D. E., T. E. GEOHEGAN, and G. H. KELLER. 1974. A two-subunit histone complex from calf thymus. *Biochem. Biophys. Res. Commun.* **59**:542.

RUBIN, R. L., and E. N. Moudrianakis. 1975. The F3-F2al complex as a unit in the self-assembly of nucleoproteins. *Biochemistry.* **14**:1718.

SAUTIERE, P., D. TYROU, B. LAINE, J. MIZON, P. RUFFIN, and G. BISERTE. 1974. Covalent structure of calf-thymus ALK-histone. *Eur. J. Biochem.* **41**:563.

SCHULZ, G. E., C. D. BARRY, J. FRIEDMAN, P. Y. CHOU, G. D. FASMAN, A. V. FINKELSTEIN, V. I. LIM, O. B. PTITSYN, E. A. KABAT, T. T. WU, M. LEVITT, B. ROBSON, and K. NAGANO. 1974. Comparison of predicted and experimentally determined secondary structure of adenylate kinase. *Nature* (*Lond.*). **250**:140.

SHIH, T. Y., and G. D. FASMAN. 1971. Circular dichroism studies of deoxyribonucleic acid complexes with arginine-rich histone IV (f2al). *Biochemistry.* **10**:1675.

SHIH, T. Y., and G. D. FASMAN. 1972. Circular dichroism studies of histone-deoxyribonucleic acid complexes. A comparison of complexes with histone I (f-1), histone IV (f2al), and their mixtures. *Biochemistry*. **11**:398.

SKANDRANI, E., J. MIZON, P. SAUTIERE, and G. BISERTE. 1967. Etude de la fraction F2b des histones de thymus de veau. *Biochimie*. **54**:1267.

SLAYTER, H. S., T. Y. SHIH, A. J. ADLER, and G. D. FASMAN. 1972. Electron microscopy and circular dichroism studies on chromatin. *Biochemistry*. **11**:3044.

SMERDON, M. J., and I. ISENBERG. 1973. The effect of temperature on histone GRK aggregation. *Biochem. Biophys. Res. Commun.* **55**:1029.

SMERDON, M. J., and I. ISENBERG. 1974. Conformational changes in histone GRK (f2al). *Biochemistry*. **13**:4046.

SNELL, C. R., D. G. SMYTH. 1975. Proinsulin: A proposed three-dimensional structure. *J. Biol. Chem.* **250**:6291.

SPERLING, R., and M. BUSTIN. 1975. Dynamic equilibrium in histone-assembly: self-assembly of single histones and histone pairs. *Biochemistry*. **14**:3332.

TUAN, D. Y. H., and J. BONNER. 1969. Optical absorbance and optical rotatory dispersion studies on calf thymus nucleohistone. *J. Mol. Biol.* **45**:59.

VAN HOLDE, K. E., and I. ISENBERG. 1975. Histone interactions and chromatin structure. *Accounts Chem. Res.* **8**:327.

VAN LENTE, F., J. F. JACKSON, and H. WEINTRAUB. 1975. Identification of specific crosslinked histones after treatment of chromatin with formaldehyde. *Cell*. **5**:45.

WAGNER, T. E. 1970. Circular dichroism study of the f2al histone in the presence of polyvinyl phosphate and DNA. *Nature (Lond.)*. **227**:65.

WAGNER, T. E., and V. VANDERGIFT. 1972. Circular dichroism studies of calf thymus Ca^{2+} nucleohistone IV. *Biochemistry*. **11**:1431.

WICKETT, R. R., H. J. LI, and I. ISENBERG. 1972. Salt effects on histone IV conformation. *Biochemistry*. **11**:2952.

WOOTTON, J. C. 1974. The coenzyme-binding domains of glutamate dehydrogenases. *Nature (Lond.)*. **252**:542.

YEOMAN, L. C., M. O. J. OLSON, N. SUGANO, J. J. JORDON, C. W. TAYLOR, W. C. STARBUCK, and H. BUSCH. 1972. Amino acid sequence of the center of the arginine-lysine-rich histone from calf thymus. The total sequence. *J. Biol. Chem.* **247**:6018.

ZICCARDI, R., and V. SCHUMAKER. 1973. Interaction of histone f2al with T7 deoxyribonucleic acid. Cooperativeity of histone binding. *Biochemistry*. **12**:3231.